Scientia Pharmaceutica

ÖSTERREICHISCHE PHARMAZEUTISCHE GESELLSCHAFT

MDPI

Article

In Silico and In Vivo Studies Reveal the Potential Preventive Impact of *Cuminum cyminum* and *Foeniculum vulgare* Essential Oil Nanocapsules Against Depression-like States in Mice Fed a High-Fat Diet and Exposed to Chronic Unpredictable Mild Stress

Karem Fouda and Rasha S. Mohamed *

Nutrition and Food Sciences Department, National Research Centre, Cairo 12622, Egypt; karemfouda@gmail.com
* Correspondence: smarasha2005@yahoo.com; Tel.: +201-55-65-26-000

Abstract

Hyperlipidemia, oxidative stress, and excessive inflammatory cytokine production are risk factors for depression. The potential preventive effects of essential oils (EOs) such as cumin and fennel EOs on depression may stem from their hypolipidemic, antioxidant, and anti-inflammatory activities. This work aimed to investigate the effects of cumin and fennel EO nanocapsules in a mouse model of depression caused by a high-fat diet (HFD) and chronic mild stress (CMS) using both in silico and in vivo studies. The cumin and fennel EOs were extracted, analyzed by GC-MS, and encapsulated in nano-form using gum Arabic and maltodextrin as wall materials. The freeze-dried nanocapsules were evaluated in HFD/CMS-treated mice. Molecular docking was used to examine the significance of the oils' compounds in blocking the active sites of hydroxymethylglutaryl-CoA (HMG-CoA) and indoleamine 2,3-dioxygenase (IDO). According to the molecular docking results, the interactions between EO components and HMG-CoA or IDO indicate that these EOs may have hypercholesterolemic and antidepressive effects. Cumin and fennel EO nanocapsules showed hypolipidemic, antioxidant, and anti-inflammatory effects in vivo. This was demonstrated by the down-regulation of oxidants (ROS, MDA, and NO) and inflammatory markers (TLR4, TNF-α, and IL-6) in the brain, changes in lipid profile parameters, and the up-regulation of antioxidant enzymes (SOD, CAT, and GSH). The in silico and in vivo outputs revealed the potential preventive impact of cumin and fennel EO nanocapsules against depression-like states in the mouse model through the prevention of dyslipidemia, neuroxidation, and neuroinflammation. More human studies are needed to fully understand the antidepressive effects of cumin and fennel EO nanocapsules.

Keywords: nanoemulsions; nanoencapsulation; essential oils; *Cuminum cyminum*; *Foeniculum vulgare*; depression

check for updates

Received: 10 July 2025
Revised: 7 August 2025
Accepted: 12 August 2025
Published: 14 August 2025

Citation: Fouda, K.; Mohamed, R.S. In Silico and In Vivo Studies Reveal the Potential Preventive Impact of *Cuminum cyminum* and *Foeniculum vulgare* Essential Oil Nanocapsules Against Depression-like States in Mice Fed a High-Fat Diet and Exposed to Chronic Unpredictable Mild Stress. *Sci. Pharm.* **2025**, *93*, 37. https://doi.org/10.3390/scipharm93030037

Copyright: © 2025 by the authors. Published by MDPI on behalf of the Österreichische Pharmazeutische Gesellschaft. Licensee MDPI, Basel, Switzerland. This article is an open access article distributed under the terms and conditions of the Creative Commons Attribution (CC BY) license (https://creativecommons.org/licenses/by/4.0/).

1. Introduction

The rising intake of high-fat fast foods, combined with rising social stress, could be a risk factor for a variety of health issues, including depression, which in turn increases the risk of diseases such as diabetes, heart disease, and stroke. High-fat diets (HFDs) change tryptophan metabolism via the kynurenine pathway (KP), which may constitute a connection between depression and inflammation. HFDs can raise pro-inflammatory cytokines that trigger the KP's first enzyme, indoleamine 2,3 dioxygenase (IDO), which activates the KP and modifies the metabolism of tryptophan. Reduced serotonin can result

from increased IDO activation, which depletes the mood-modulating neurotransmitter [1]. HFDs combined with chronic unpredictable mild stress (CUMS), which mimics social stress, can promote depression and associated comorbidities by activating Toll-like receptors 4 (TLR4) in the gut and central nervous system, resulting in cytokine overproduction [2]. The blood–brain barrier (BBB) allows pro-inflammatory cytokines to enter or be produced in the brain via active transport, "leaky" areas across the BBB and the afferent vagal pathway, or activated monocytes, which can produce second messenger signals that cause glial cells to overproduce cytokines. Cervellati et al. [3] report that unusually increased cytokine levels affect neurotransmission, the HPA axis, hippocampal neurogenesis, and other brain structures and functions. HFDs and the disturbance of lipid metabolism cause gut microbial dysbiosis and a marked decrease in healthy gut microbial products [4]. Through the microbiota–gut–brain axis, the dysbiosis of gut microbes influences the regulation of brain function and the behavior of the central nervous system [5]. Additionally, depression may arise as a result of oxidative stress brought on by an HFD and CUMS, which also increase oxidant formation and disrupt the functions of antioxidant enzymes. Elevated reactive oxygen species (ROS) and inflammatory biomarkers stimulate further oxidative stress and neuroinflammation, ultimately resulting in cellular demise, perhaps contributing to depression [6].

Essential oils (EOs) are recognized for their capacity to scavenge free radicals, which contributes to their antioxidant action. This action motivates their application in the treatment of numerous diseases, including cancer, neurological disorders, cardiovascular disorders, and immune system disorders, as well as in food preservation [7]. Because essential oils' components can pass across the blood–brain barrier and interact with biological receptors linked to depression, they have long been used to treat the symptoms of depression [8,9]. The cumin plant (*Cuminum cyminum*), a member of the Apiaceae family, is an annual herbaceous plant [10]. The greenish-brown seeds of cumin are native to Iran, Egypt, and the Mediterranean region [11]. The most significant chemical component of cumin is its essential oil, which exhibits strong antioxidant activity and has high concentrations of phenol chemicals, primarily cuminaldehyde and para-cymene [12]. It has been demonstrated that cumin EO has anti-inflammatory activity and that it inhibits the mRNA expression of inflammatory factors such as interleukin (IL)-1β and IL-6 [13]. It was found that cumin EO reduced blood lipids in pre-diabetic patients [14]. Haque and Ansari [15] demonstrated that cumin-derived cuminaldehyde reduced cholesterol, triglycerides, and high-density lipoprotein in the serum and liver of rats fed a high-fat diet, suggesting the hypocholesterolemic effect of cumin EO. The fennel plant (*Foeniculum vulgare*), a member of the Apiaceae (Umbelliferae) family, is used medicinally. Fennel essential oil also possesses antioxidant and anti-inflammatory properties [16]. Numerous phytochemical studies on the chemical constitution of fennel essential oil from various sources have revealed that a-pinene, fenchone, anethole, and estragol are among its main constituents [17]. It was discovered that fennel EO lowered cholesterol, triglycerides, and high-density lipoprotein in the serum of rats fed a high-fat diet and may play a function in the modulation of the central and autonomic nervous systems [18]. According to [19], fennel affects the central nervous system by increasing the total neurotransmitter content, while its antioxidant properties protect against stress and stress-related disorders [20].

Encapsulation effectively protects EO ingredients from chemical reactions and unfavorable interactions with other food components; it improves their solubility, reduces migration, and maintains bioactive stability during processing and storage. Furthermore, encapsulation is thought to help manage the release of encapsulated chemicals, as well as their bio-accessibility and bioavailability [21]. Nanoencapsulation has been shown to

improve the properties of EOs in a variety of industrial processes. As a result, in this study, nanoencapsulation was used to develop nanocapsules of cumin and fennel EOs.

Lipid reduction and alterations in oxidative and inflammatory markers may be implicated in the antidepressant response. Therefore, it was postulated that the nanoencapsulated forms of cumin and fennel EOs could prevent depression through their lipid-lowering, antioxidant, and anti-inflammatory activities. The primary goal of this study was to assess the effects of cumin and fennel EO nanocapsules on depression-like states in mice induced by CUMS and a HFD. Characterizing these nanocapsules was the secondary goal.

2. Materials and Methods

2.1. Raw Materials and Chemicals

Cumin and fennel seeds were acquired at a local market (Haraz in Cairo, Egypt). Arabic gum and maltodextrin were purchased from Loba Chemie in Mumbai, India. Sigma-Aldrich supplied DPPH (1,1-diphenyl-2-picrylhydrazyl, Cat N: D9132-1G). The ingredients used in preparing the animal diets were purchased from a local market in Egypt. Cholesterol (≥99%, Cat N: C8667-25G) and ascorbic acid (Cat N: A92902-25G) were purchased from Sigma-Aldrich (St. Louis, MO, USA). ELISA kits were purchased from Sunlong Biotech Co., Ltd. (Hangzhou, China). All chemicals and reagents used in this study were of high analytical quality.

2.2. Methods

2.2.1. Essential Oil Preparation

The hydrodistillation technique, carried out using Clevenger apparatus, was used to extract the EOs from cumin and fennel seeds. Water contaminants were eliminated from the extracted EOs by passing the oil through anhydrous Na_2SO_4. The EOs were stored at 4 °C in a clean dark glass vial for further investigation.

2.2.2. Gas Chromatography–Mass Spectrometry (GC-MS) Analysis

The analysis was carried out using a gas chromatography system (Agilent 8890 GC System, Santa Clara, CA, USA) connected to a mass spectrometer (Agilent 5977B GC/MSD) and an HP-5MS fused silica capillary column (30 m, 0.25 mm i.d., and 0.25 mm film thickness). The oven temperature was originally set to 50 °C, and scheduled to rise to 220 °C at a rate of 5 °C/min, and then to 280 °C at a rate of 15 °C/min, before remaining at 280 °C for 7 min. Helium was employed as the carrier gas, with a flow rate of 1.1 mL/minute. The essential oil was diluted in diethyl ether (30 µL essential oil/mL diethyl ether), and 1 µL of the solution was injected into the GC with a split ratio of 1:50. The injection temperature was 230 °C. Mass spectra in the electron impact mode (EI) were obtained at 70 eV, with the scan m/z ranging from 39 to 500 amu. The isolated peaks were found by cross-referencing them with mass spectrum data from the National Institute of Standards and Technology's library (NIST 17).

2.2.3. In Silico Assays of the Potential Inhibition of Indoleamine 2,3-dioxygenase and Hydroxymethylglutaryl-CoA

Molecular Docking

The 3D crystal structures [22] of the human indoleamine 2,3-dioxygenase (PDB: 6E45) and hydroxymethylglutaryl-CoA [23] (PDB: 1DQ9) proteins were downloaded from the RCSB Protein Data Bank database (https://www.rcsb.org/, accessed on 10 March 2024). The IDO protein contains 4 chains (A, B, C and D) and the resolution equals 2.00 A. The HMG-CoA protein contains 4 chains (A, B, C and D) and the resolution equals 2.80 A. The PubChem database (https://pubchem.ncbi.nlm.nih.gov/ accessed on 10 March 2024)

was used to obtain the 3D chemical structures (SMILE code) of the bioactive molecules cuminaldehyde (CID: 326), terpinen-7-al (CID: 526762), and trans-anethole (CID: 637563), as well as indoximod (as IDO inhibitor, CID:) and fluvastatin (as HMG-CoA inhibitor, CID:). PyRx software (free version 3.12.2) was used to determine the binding affinity score of cumin and fennel EO bioactive molecules to the IDO and HMG-CoA proteins. The target proteins and ligands were loaded onto the PyRx software, and then minimized and converted to PDBQT [24]; the GRID parameters were maximized (center x: 42.7962; y: 49.0390; z: 29.0814, and dimension (angstrom) x: 100.9030; y: 115.5853; z: 99.1823, for the IDO protein; center x: 7.4730; y: 15.639; z: 13.5675, and dimension (angstrom) x: 82.7190; y: 111.186; z: 102.6082, for the HMG-CoA protein), and then a blind docking study was performed [25]. Protein and ligand complexes were visualized using PyMOl (free version 2.5.5) and Discovery Studio software (free version 2021).

Normal Mod Analysis

Normal mod analysis (NMA) was employed to evaluate protein–ligand complex stability. The iMODS server (http://imod.chaco.nlab.org, accessed on 10 March 2024) was used to perform MD simulations [26]. While the other parameters were left at their default settings, the simulation time was changed to 10 ns. The iMODS server was used to analyze docking complexes' structural dynamics and determine their molecular mobility. Protein–ligand complexes' stability was assessed using deformability, B-factor, eigenvalue, variance, covariance map, and elastic network analysis. The input files were docked PDB files and submitted to the iMODS server with default parameters.

2.2.4. Fabrication of EO Nanocapsules

According to the technique described by Mahdi et al. [27], cumin and fennel EO nanoemulsions were prepared. Because Arabic gum and maltodextrin may protect volatile components, improve stability, and regulate release, they are frequently utilized as wall materials in the encapsulation of essential oils. These materials have advantages such as increased bioavailability, stability, and encapsulation efficiency [28]. Arabic gum (15.0% w/v) was hydrated in deionized water at 4 °C for an entire night. Maltodextrin (15.0% w/v) was added to the gum solution, and then Tween 80 (1.0% w/v, based on water) was added to help form the emulsion. To the aqueous solution, a precise volume of oil (10 g) was added drop by drop. A high-speed homogenizer (Ingenieurbüro CAT, Ballrechten-Dottingen, Germany) was used to homogenize the mixture for five minutes at 10,000 rpm. Using an ultrasonicator (vibra cell; Sonics & Materials, Inc., Newtown, CT, USA), the nanoencapsulated EOs of cumin and fennel were produced. To obtain a homogeneous suspension, sonication with amplitude level of 60% for one second and rest for one second in an ice bath for four minutes were employed. The nanoemulsions were freeze-dried right away using a freeze dryer (ALPHA 1-4 LSC, Osterode, Germany) for 48 h at −52 °C. The dried cumin and fennel EO nanocapsules were kept at 4 °C for further investigation.

2.2.5. Measurement of Particle Size, Polydispersity Index, and Zeta Potential

Zetasizer (Santa Barbara, CA, USA) was used to assess the particle size distribution, polydispersity index (PDI), and zeta potential at 25 ± 0.1 °C. The nanoemulsion was diluted with distilled water at a ratio of 1:10 v/v. After this, gentle sonication was applied to the mixture. One milliliter (mL) of the diluted nanoemulsion was used for measurements after it had been moved to a disposable PVC clear cuvette.

2.2.6. Encapsulation Efficiency Determination

According to the method described by Dwivedy et al. [29], the encapsulation efficiency (EE) was determined using a UV-Vis spectrophotometer (Jasco V-730, serial No. A 112361798, Tokyo, Japan). The amount of oil loaded into the freeze-dried nanocapsules was calculated by extracting the oil from 10 mg of the freeze-dried nanocapsules using 3 mL of ethyl acetate (99.5%) and comparing its absorbance to a standard curve made for the essential oils at 259 nm. The EE was calculated using Equation (1):

$$EE\ (\%) = \frac{Total\ amount\ of\ oil\ in\ nanocapsules}{Initial\ amount\ of\ the\ oil} \times 100 \quad (1)$$

2.2.7. Antioxidant DPPH and FRAP Assays

DPPH Free Radical Scavenging Activity Assay

Using the method described by Asres et al. [30], DPPH activity was assessed. Four milligrams of DPPH were dissolved in one hundred milliliters of 80% methanol to create a DPPH stock solution (0.04 mg/mL). A 3.9 mL volume of DPPH solution (in 80% methanol) was mixed with an 100 µL aliquot of each sample and ascorbic acid standards at different concentrations. After that, these mixes were allowed to sit at room temperature for 30 min in the dark. A UV-Vis spectrophotometer (Jasco V-730, serial No. A 112361798, Tokyo, Japan) was then used to measure the absorbance of each reaction mixture (samples and ascorbic acid standards) at 517 nm. Equation (2) was then used to determine the scavenging activity, which was represented as % inhibition:

$$inhibition\ (\%) = \frac{A1 - A2}{A1} \times 100 \quad (2)$$

where A1 indicates the absorption of the blank sample, and A2 indicates the absorption of tested sample solution. The DPPH radical scavenging activity of the sample was expressed as mg ascorbic acid equivalents/g freeze-dried nanocapsules.

Ferric Reducing Antioxidant Power (FRAP) Assay

The ferric reduction capacity of the fennel and cumin oils was measured using the method described by Asres et al. [30]. A freshly prepared FRAP reagent solution consisting of 25 mL of 0.3 M acetate buffer, 40 mM HCl, and 2.5 mL of 20 mM $FeCl_3 \cdot 6H_2O$ was mixed with around 100 µL of the sample aliquot. After that, the mixture was incubated for 30 min at 37 °C in a water bath. A UV-vis spectrophotometer (Jasco V-730, serial No. A 112361798, Tokyo, Japan) was used to determine the absorbance at 593 nm. A standard curve for the concentration of the ascorbic acid and the FRAP reducing power rate was plotted. The FRAP reducing power of the sample was expressed as mg ascorbic acid equivalents/g freeze-dried nanocapsules.

2.2.8. Release of the EO at Gastrointestinal pH

The pH conditions of intestinal and stomach fluids were simulated [31] by mixing 30 mg of the freeze-dried nanocapsules with 7 mL of phosphate-buffer solution (PBS) at 2.5 and 6.5, respectively. Four milliliters of ethanol was added in order to make the EO more soluble. At regular intervals, the suspension was incubated at 37 °C and 100 rpm. The aliquots (1 mL) that were removed from the suspension were filtered. At a wavelength of 232.4 nm, a UV-Vis spectrophotometer was used to measure the amount of released EO. The cumulative amount of released EO was calculated using Equation (3):

$$Cumulative\ release\ (\%) = \frac{Mx}{Mo} \quad (3)$$

where Mx and Mo are the amount of the EO released and the amount of the EO in the capsules initially, respectively.

2.2.9. Scanning Electron Microscopy (SEM)

A high-resolution scanning electron microscopy (SEM) model (TESCAN VEGA 3 with a field emission gun, Brno-Kohoutovice, Czech Republic) was utilized to investigate the morphological structure of the freeze-dried EO nanocapsules. The samples were coated with gold for 60 s using a Quorum Q 150 ES (Quorum Technologies, Oxford, UK).

2.2.10. Bioassays

Experimental Animals

Adult male white albino mice (40 mice, 8 months of age) weighing 30–40 g were obtained from the National Research Centre animal house in Cairo, Egypt. Each group (n = 10) was housed in a stainless steel cage. The feeding environment was maintained at a consistent temperature (23 ± 2 °C) and relative humidity (45–50%), and had a light/dark cycle of 12 h.

Diets

Diets were prepared in the nutrition and food sciences department, National Research Centre, Egypt. Animals were fed either an AIN-93 balanced diet (58.5% maize starch, 5% fiber, 3.5% corn oil, 10% sucrose, 12% casein-supplemented protein, 3.5% AIN-93 salt mixture, and 1% AIN-93 vitamin mixture) prepared as described by Mohamed et al. [32], or a high-fat diet (37.5% maize starch, 35% lard, 1% cholesterol, 10% sucrose, 12% casein-supplemented protein, 3.5% AIN-93 salt mixture, and 1% AIN-93 vitamin mixture) prepared according to Lippi [33]. Food and water were freely available to the mice. The animals were weighed weekly throughout the study to monitor weight changes. Food intake was also monitored throughout the trial. Due to group living, the average intake per mouse was determined as [(daily food consumed)/Number of animals in the cage].

Chronic Mild Stress (CMS)

According to the method described by Lippi [33], the animals were exposed to CMS, and the stressors were modified and modeled. Over four weeks of stress exposure, the order of stressors was given at random. Every week, the mice were subjected to four days of stressors, two on each day. The two stressors, one of which occurred in the first half of the light cycle and the other in the second half, were assigned at random. The stressors included swimming in cold water (8–10 °C) for 5 min, bright-light/open-field exposure (10 min), soaking the animals' bedding in water and leaving them in the cage for 2 h, removing the bedding and placing the mice in an empty cage for 2 h, and adjusting the light cycle during the dark phase.

The Design of the Animal Experiment

According to the diagram (Figure 1), mice were acclimatized for one week before being divided into four groups (n = 10 per group). The control normal (CN) group was fed a balanced diet and given 1 mL of distilled water orally. The second group (HFD/CMS), the positive control, was fed a high-fat diet, exposed to CMS, and given 1 mL of distilled water orally. The third group (cumin oil nanocapsules, CON) was fed an HFD, exposed to CMS, and orally given 1 mL of distilled water containing 8 mg of freeze-dried cumin oil nanocapsules (equal to 50 mg of oil per kg of body weight). The fourth group (fennel oil nanocapsules, FON) was fed an HFD, exposed to CMS, and orally given 1 mL of distilled water containing 8 mg of freeze-dried fennel oil nanocapsules (equal to 50 mg of oil per kg of body weight). The dose of EOs was selected according to the studies of Moubarz et al. [34]

and Asaad et al. [35]. As a dietary supplement, this dosage has demonstrated antioxidant and anti-inflammatory properties. The treatment period lasted for 28 consecutive days. Food intake was recorded daily. Body weight gain or loss was calculated as follows: body weight gain or loss = [body weight at the end of the experiment-body weight at the beginning of the experiment].

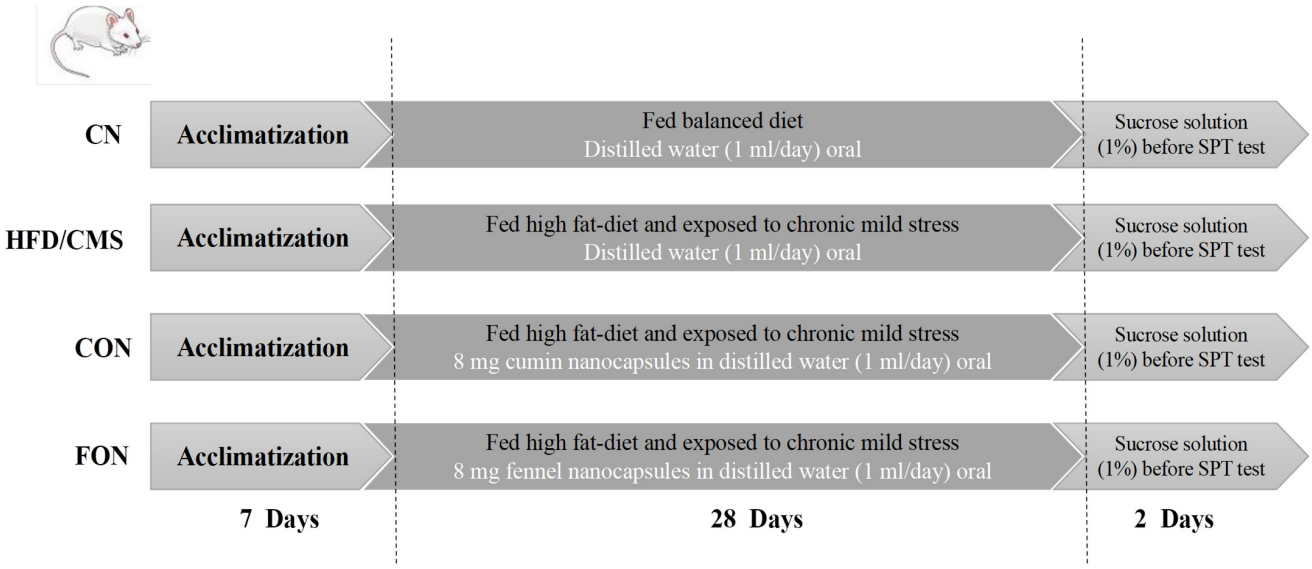


Figure 1. A schematic diagram of the animal experiment design.

All experiments were carried out according to research protocols approved by the Medical Research Ethics Committee (MREC) at the National Research Centre, which are in accordance with the provisions of the relevant Egyptian laws and with the Helsinki Declaration, as well as the Institutional Animal Care and Use Committee (IACUC) guidelines and recommendations and WHO rules regarding the ethics of scientific research. Approval Certificate No. 180572022.

Sucrose Preference Test

The test used to assess an animal's preference for pleasure is called the sucrose preference test (SPT). This test was conducted to determine whether exposure to an HFD and CMS caused anxious or depressive-like behavior, as well as to determine the potential preventive effect of the EO nanocapsules. The SPT was performed right away following a 4-week HFD and CMS exposure period. First, mice were given two bottles of sucrose solution and given 48 h to acclimatize to the consumption of 1% sucrose. The mice were denied food and drink for twelve hours before the test. To conduct the SPT, each mouse was housed in a different cage and given two pre-weighed bottles, one of which contained 1% sucrose solution and the other drinking water. The bottles were weighed an hour later, and the volume of water or sucrose solution that had been drunk was noted. To determine whether distinctive anhedonia was present, the percentage preference for sucrose was calculated [36].

Blood Collection

The animals were sacrificed through decapitation under sodium pentobarbital anesthesia at a dose that did not interfere with the biochemical measurements (50 mg/kg, i.p.) [37], and their blood was collected from the body trunk in EDTA-free tubes before being centrifuged (3000 rpm; 10 min). All serum samples were kept at −80 °C for analysis.

Tissues Collection

The brain of each animal was removed to make homogenates (10% w/v) in a cold homogenization buffer (100 mM potassium phosphate buffer, pH 7.4). After centrifuging the homogenates, the supernatants were utilized to carry out the biochemical analysis.

Biochemical Analysis of the Brain and Serum

Using ELISA kits (Sunlong Co., Ltd. China) in accordance with the manufacturer's instructions, the brain levels of acetylcholinesterase (AChE), dopamine (DA), 5-hydroxytryptamine (5-HT), tumor necrosis factor-alpha (TNF-α), interleukin 6 (IL-6), Toll-like receptors 4 (TLR4), and reactive oxygen species (ROS) were determined. Using the colorimetric techniques, the levels of malondialdehyde (MDA), reduced glutathione (GSH), superoxide dismutase (SOD), nitric oxide (NO), and catalase (CAT) in the brain were measured as described previously by [38]. The serum of each mouse was colorimetrically analyzed for total cholesterol (T. Ch), high-density lipoprotein cholesterol (HDL-Ch), low-density lipoprotein cholesterol (LDL-Ch), triglycerides (TGs), alkaline phosphatase (ALP), lactate dehydrogenase (LDH), aspartate transaminase (AST), alanine transaminase (ALT), creatinine, urea, and albumin as described previously by [32]. The ratio of total cholesterol levels to HDL-Ch, non-HDL-Ch, and VLDL levels were calculated.

Statistical Analysis

Statistical analysis was carried out using SPSS software version 21 (IBM SPSS Inc., Chicago, IL, USA). The results were provided as the mean ± standard error (SE) and statistically evaluated using one-way ANOVA and the Duncan test. A difference was considered statistically significant at $p < 0.05$.

3. Results and Discussion

3.1. The Composition of Cumin and Fennel EOs

The quality of the sample and many geographic and climatic factors influence the chemical profile of essential oils. So, before assessing the possible bioactivity of the cumin and fennel essential oils, their chemical composition was determined. Hydrodistillation of the cumin seeds produced 3% (w/w) clear yellowish liquid oil, whereas that of the fennel seeds produced 4% (w/w). Six and sixteen distinct compounds, respectively, were identified by GC–MS analysis of the fennel and cumin oils (Figure 2A,B). The isolated peaks were identified by matching the retention time (RT) with data from the library of mass spectra (National Institute of Standards and Technology, NIST 17). The primary constituents of cumin EO (Table 1) were cuminaldehyde (26.48%), γ-terpinen-7-al (19.32%), α-terpinen-7-al (13.87%), γ-terpinene (11.02%), and p-cymene (7.94%). The primary constituents of fennel EO (Table 2) were trans-anethole (81.46%), D-limonene (11.16%), and L-fenchone (4.48%). The results obtained are generally in line with Moradi et al. [39] and Stefănescu et al. [40], who found that the major compounds in cumin EO were cuminaldehyde (27.99%), p-cymene (17.31%), and γ-terpinene (16.67%), while those in fennel EO were trans-anethole (64.6%) and fenchone (24.5%).

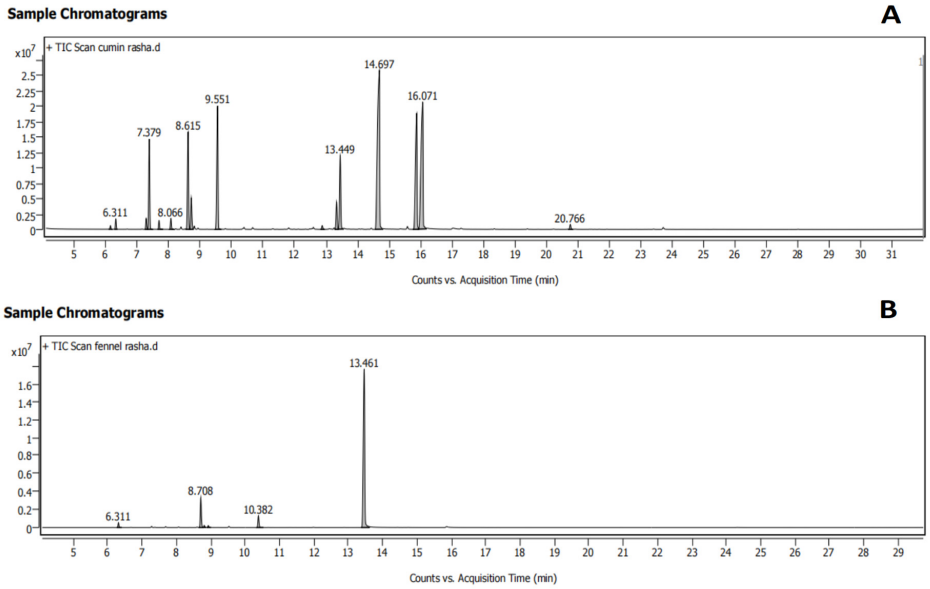


Figure 2. GC-MS chromatogram of cumin (**A**) and fennel (**B**) EOs.

Table 1. Cumin EO constituents (%).

Retention Time (min)	Compound	Chemical Formula	Molecular Weight (g/mol)	%
6.143	α-Thujene	$C_{10}H_{16}$	136.23	0.22
6.311	α-Pinene	$C_{10}H_{16}$	136.23	0.64
7.281	β-Phellandrene	$C_{10}H_{16}$	136.23	0.72
7.379	β-Pinene	$C_{10}H_{16}$	136.23	6.67
7.685	β-Myrcene	$C_{10}H_{16}$	136.23	0.58
8.066	α-Phellandrene	$C_{10}H_{16}$	136.23	0.74
8.615	p-Cymene	$C_{10}H_{14}$	134.22	7.94
8.713	D-Limonene	$C_{10}H_{16}$	136.23	2.41
9.551	γ-Terpinene	$C_{10}H_{16}$	136.23	11.02
12.877	Terpinen-4-ol	$C_{10}H_{18}O$	154.25	0.3
13.334	3-p-Menthen-7-al	$C_{10}H_{16}O$	152.23	2.18
13.449	Estragole	$C_{10}H_{12}O$	148.2	6.49
14.697	Cuminaldehyde	$C_{10}H_{12}O$	148.2	26.48
15.880	α-Terpinen-7-al	$C_{10}H_{14}O$	150.22	13.87
16.071	γ-Terpinen-7-al	$C_{10}H_{14}O$	150.22	19.32
20.766	Acoradiene	$C_{15}H_{22}O$	218.33	0.42

Table 2. Fennel EO constituents (%).

Retention Time (min)	Compound	Chemical Formula	Molecular Weight (g/mol)	%
6.311	α-Pinene	$C_{10}H_{16}$	136.23	1.5
8.708	D-Limonene	$C_{10}H_{16}$	136.23	11.16
8.806	Eucalyptol	$C_{10}H_{18}O$	154.25	0.73
8.921	trans-β-Ocimene	$C_{10}H_{16}$	136.23	0.68
10.382	L-Fenchone	$C_{10}H_{16}O$	152.23	4.48
13.461	Trans-Anethole	$C_{10}H_{12}O$	148.2	81.46

3.2. Findings of the In Silico Studies

Molecular docking is a promising computational assay that simulates the potential binding status, complexation, and ligand–receptor interactions [41]. Hypercholesterolemia has been linked to depression and reduced brain functioning because a fat- and cholesterol-rich diet affects the BBB, resulting in neuroinflammation and cognitive impairment [42]. Therefore, one of the goals of the current study was to investigate the cholesterol-lowering

effect of cumin and fennel EO nanocapsules, both in vivo and in silico, by investigating the possibility of inhibiting HMG-CoA reductases, the rate-limiting enzyme in cholesterol biosynthesis. Indoleamine 2,3-dioxygenase catalyzes the first and rate-limiting step in the conversion of L-tryptophan to N-formyl kynurenine indoleamine. One approach to treating depression is to directly target kynurenine synthesis and reduce its downstream neurotoxic metabolites. As a result, the easiest method is to avoid the accumulation of kynurenine metabolites by reducing IDO activity with enzyme inhibitors [43]. IDO inhibitors have been identified as promising therapeutic targets for depressive disorders. Molecular docking was performed between the IDO and HMG-CoA proteins and the primary compounds in cumin and fennel EOs to anticipate the possibility of EO components blocking the binding sites on these enzymes and thus potentially disrupting their function. Figure 3 displays the 2D interactions of IDO and its inhibitor indoximod, as well as HMG-CoA and its inhibitor fluvastatin. Figures 4–9 display the outputs of molecular docking and normal mod analysis for IDO-cuminaldehyde, IDO-terpinen-7-al, IDO-trans-anethole, HMG-CoA-cuminaldehyde, HMG-CoA-terpinen-7-al, and HMG-CoA-trans-anethole, respectively. According to Table 3, compared to indoximod and fluvastatin as inhibitors of IDO and HMG-CoA, terpinen-7-al recorded a high binding affinity with both HMG-CoA and IDO, and trans-anethole interacted with the active sites of the HMG-CoA and IDO receptors via both hydrophobic interactions and a hydrogen bond. However, more research on the other components is needed. It has been suggested that masking the residues on active sites is a useful tactic to inhibit enzymes [44]. The presence of both hydrophobic interactions and hydrogen bonds, as reported by Noshad et al. [45], suggests a potentially stronger and more specific interaction. This could have implications for the ligand's binding affinity and therapeutic potential as an enzyme inhibitor that blocks the receptors of the enzyme. Thus, inhibiting IDO prevents the conversion of L-tryptophan to N-formyl kynurenine indoleamine, and inhibiting HMG-CoA reductase, which is required by the body to produce cholesterol, reduces the amount of cholesterol in the bloodstream.

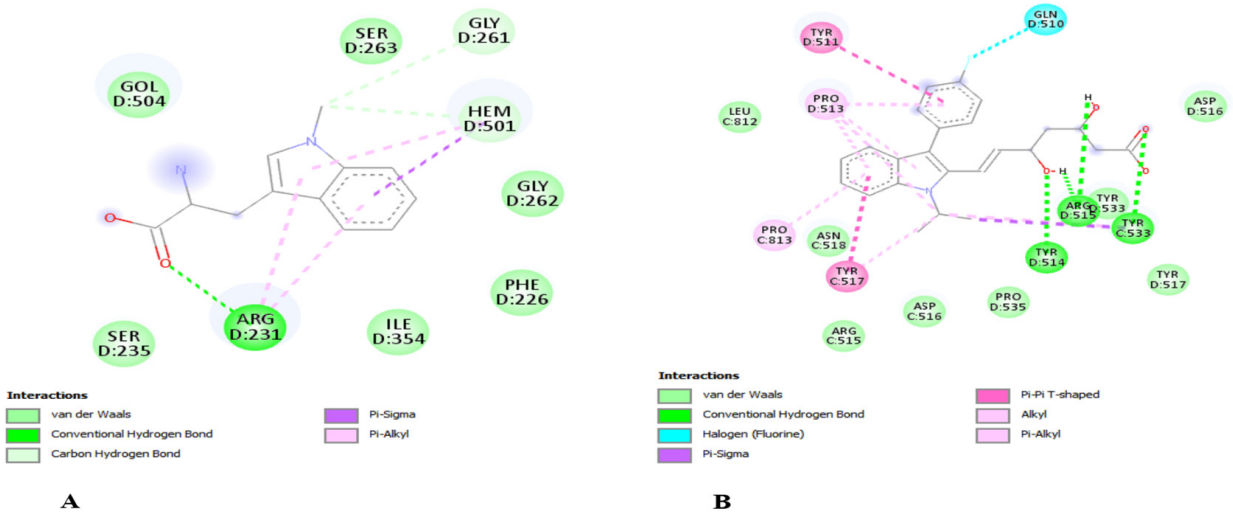


Figure 3. The 2D interactions of the IDO-indoximod complex (**A**) and HMG-CoA-fluvastatin (**B**).

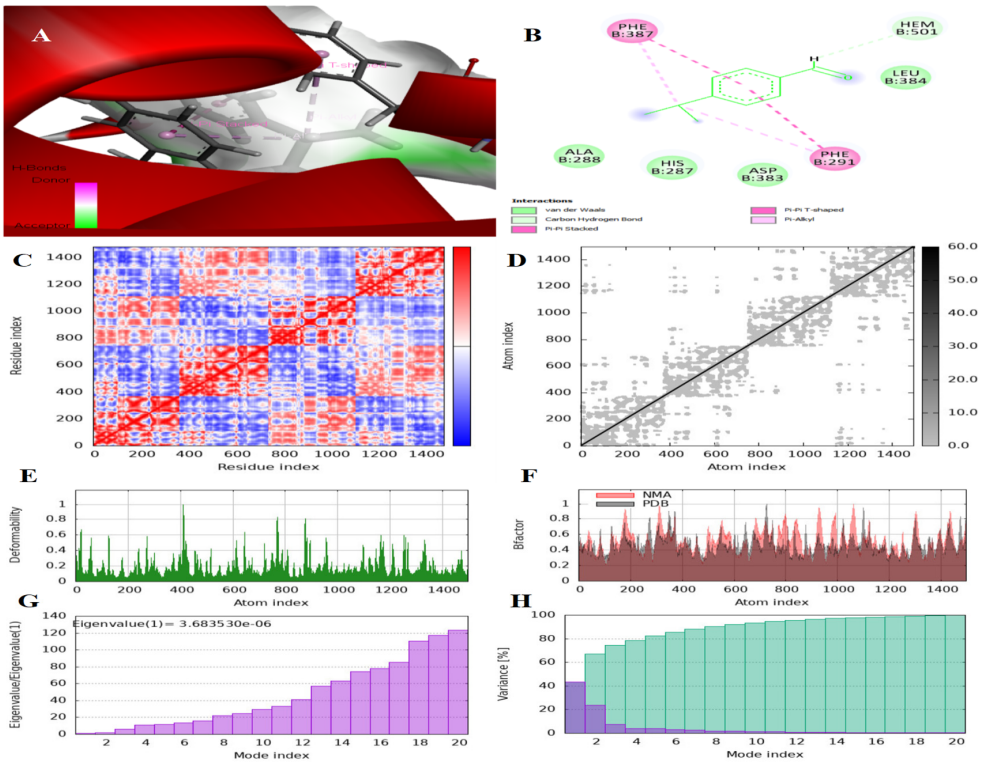


Figure 4. The outputs of molecular docking and normal mod analysis for the IDO-cuminaldehyde complex. (**A**) The 3D interaction; (**B**) the 2D interaction; (**C**) elastic network model; (**D**) covariance map; (**E**) deformability; (**F**) B-factor plot; (**G**) eigenvalue plot; (**H**) variance plot.

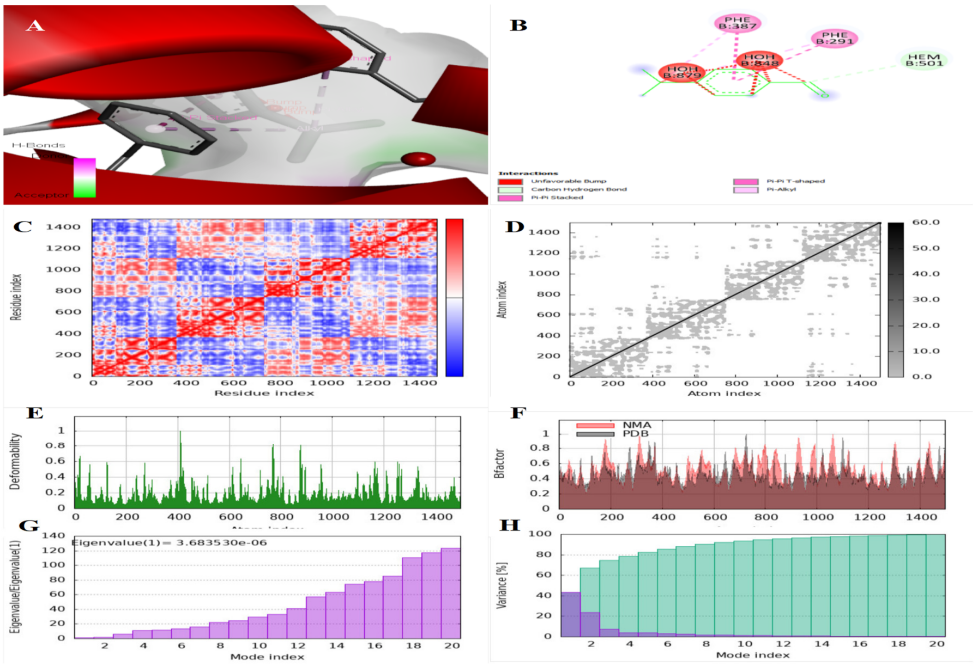


Figure 5. The outputs of molecular docking and normal mod analysis for the IDO-terpinen-7-al complex. (**A**) The 3D interaction; (**B**) the 2D interaction; (**C**) elastic network model; (**D**) covariance map; (**E**) deformability; (**F**) B-factor plot; (**G**) eigenvalue plot; (**H**) variance plot.

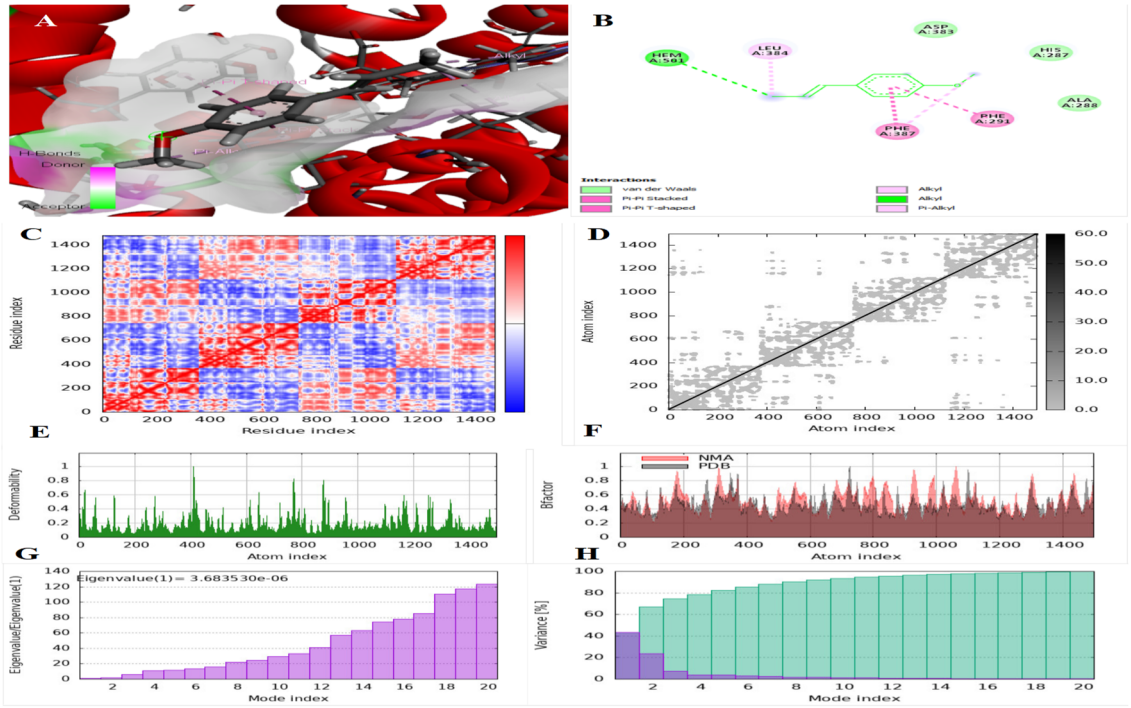


Figure 6. The outputs of molecular docking and normal mod analysis for the IDO-trans-anethole complex. (**A**) The 3D interaction; (**B**) the 2D interaction; (**C**) elastic network model; (**D**) covariance map; (**E**) deformability; (**F**) B-factor plot; (**G**) eigenvalue plot; (**H**) variance plot.

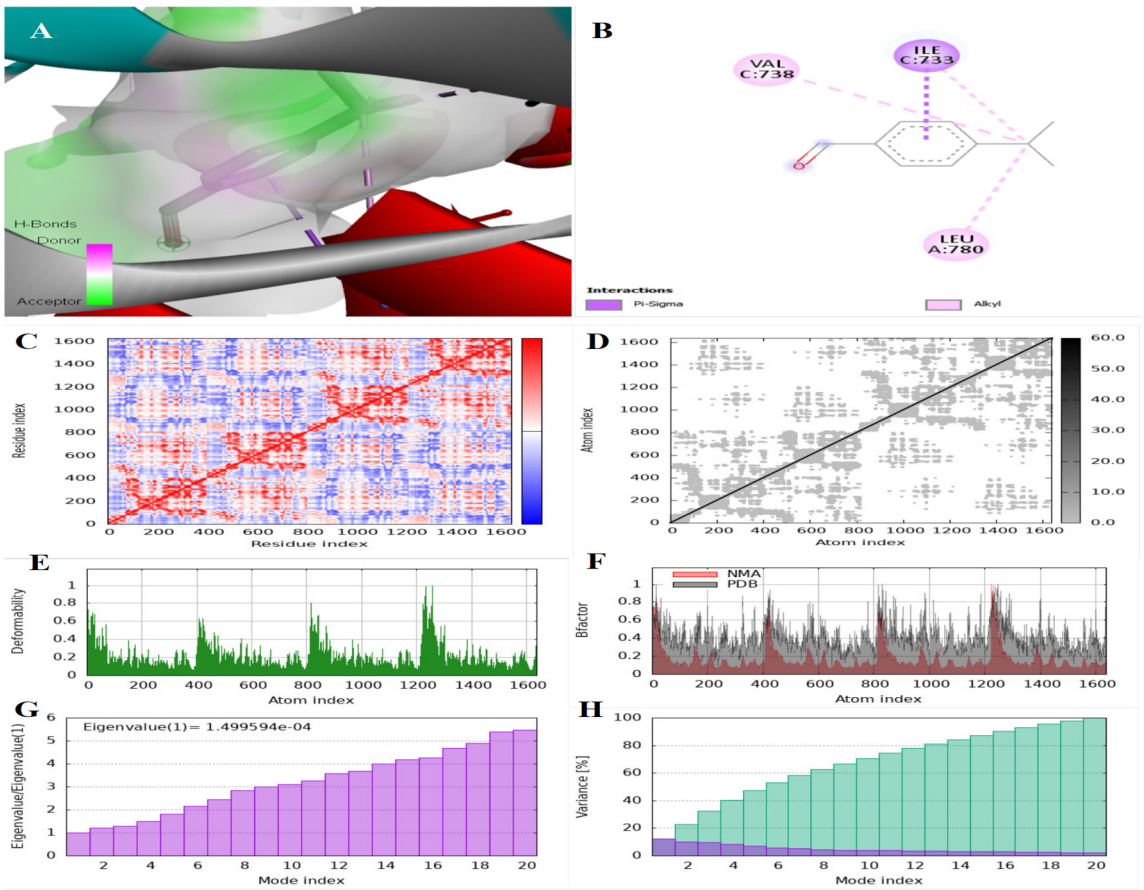


Figure 7. The outputs of molecular docking and normal mod analysis for the HMG-CoA-cuminaldehyde complex. (**A**) The 3D interaction; (**B**) the 2D interaction; (**C**) elastic network model; (**D**) covariance map; (**E**) deformability; (**F**) B-factor plot; (**G**) eigenvalue plot; (**H**) variance plot.

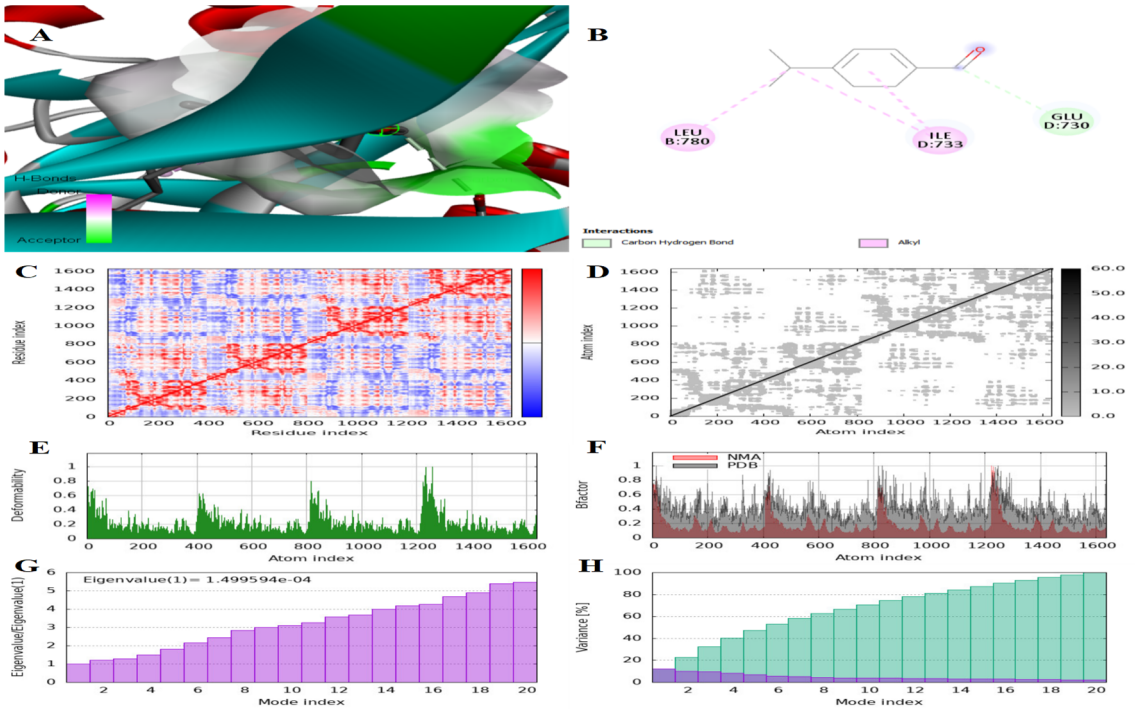


Figure 8. The outputs of molecular docking and normal mod analysis for the HMG-CoA-terpinen-7-al complex. (**A**) The 3D interaction; (**B**) the 2D interaction; (**C**) elastic network model; (**D**) covariance map; (**E**) deformability; (**F**) B-factor plot; (**G**) eigenvalue plot; (**H**) variance plot.

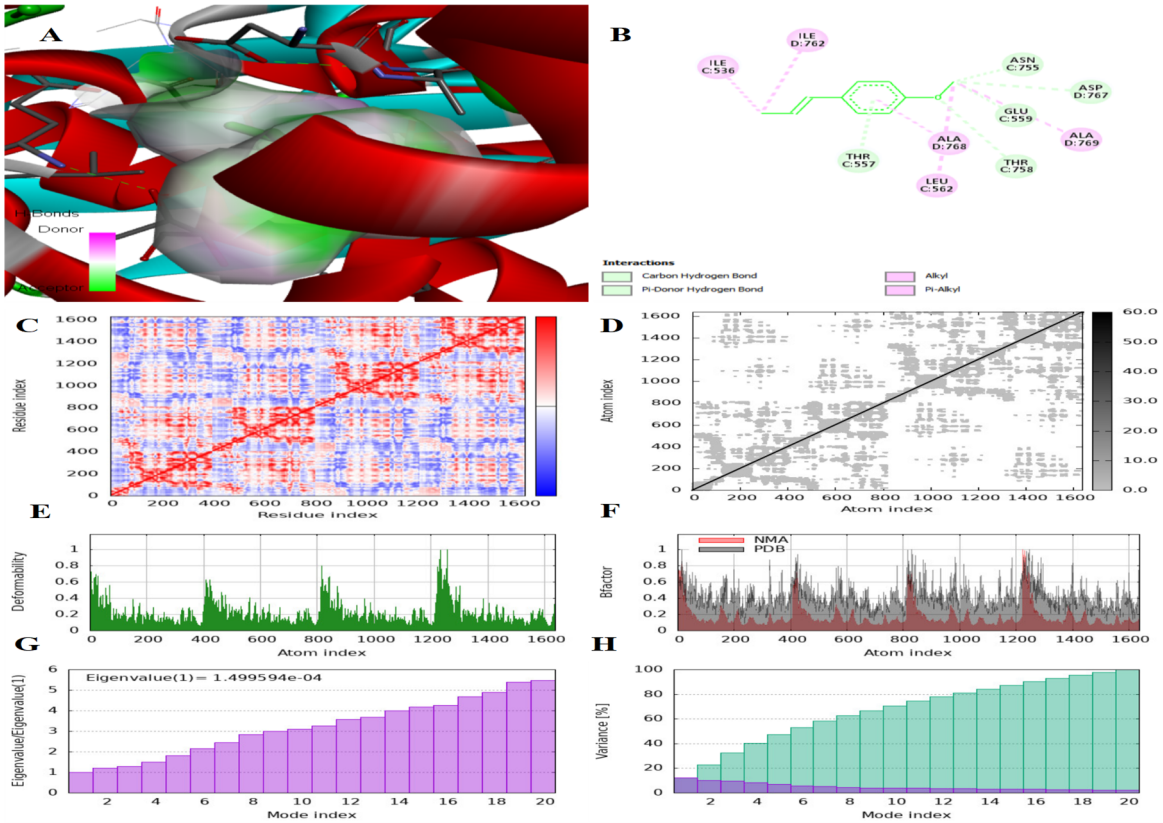


Figure 9. The outputs of molecular docking and normal mod analysis for the HMG-CoA-trans-anethole complex. (**A**) The 3D interaction; (**B**) the 2D interaction; (**C**) elastic network model; (**D**) covariance map; (**E**) deformability; (**F**) B-factor plot; (**G**) eigenvalue plot; (**H**) variance plot.

Table 3. Binding affinity and interactions between EO molecules and target proteins.

Protein	Ligand	Binding Affinity (kcal/mol)	Interactions	
			Hydrogen Bonds	Hydrophobic Interaction
IDO	Cuminaldehyde	−6.3	(1) at HEM 501 residue	(2) at PHE 291 and PHE 387 residues
	Terpinen-7-al	−9.9	(1) at HEM 501 residue	(2) at PHE 291 and PHE 387 residues
	Trans-anethole	−5.9	(1) at HEM 501 residue	(3) at PHE 291, PHE 387, and LEU 384 residues
	Indoximod	−6.2	(1) at ARG 231 residue	-
HMG-CoA	Cuminaldehyde	−5.9	(3) at ILE 733, VAL 738, and LEU 780 residues	-
	Terpinen-7-al	−8.5	(1) at GLU 730 residue	(2) at ILE 733 and LEU 780
	Trans-anethole	−5.7	(5) at THR 557, THR 758, GLU 559, ASN 755, and ASP 767 residues	(5) at ILE 536, ILE 762, LUE 562, ALA 768, and ALA 769 residues
	Fluvastatin	−8.2	(3) at TYR 514, ARG 515, and TYR 533 residues	(4) at TYR 511, PRO 513, TYR 517, and PRO 813 residues

The iMODS server was used to run normal mod analysis (NMA) in order to assess the docked complexes' physical movements and stability. The slow dynamics of the free IDO and HMG-CoA proteins and docked complexes were examined, and their large-amplitude conformational changes were demonstrated, using NMA. iMODS is a quick and easy tool for determining a protein's flexibility. Using NMA, which is integrated with the docked complex's coordinates, it examines both molecular motion and structural flexibility. The foundation of NMA of proteins is the idea that the maximal movements in a protein that are functionally significant are indicated by the vibrational normal modes that exhibit the lowest frequencies [46]. The covariance matrices of the IDO-cuminaldehyde (Figure 4C), IDO-terpinen-7-al (Figure 5C), IDO-trans-anethole (Figure 6C), HMG-CoA-cuminaldehyde (Figure 7C), HMG-CoA-terpinen-7-al (Figure 10C), HMG-CoA-trans-anethole (Figure 9C), free IDO (Figure 9A), and free HMG-CoA (Figure 11A) complexes show the relationships between a complex's residues. While the white hue in the matrix denotes uncorrelated motion, the red color shows a respectable correlation between residues. Additionally, the blue hue exhibits anti-correlations. The quality of the complex increases with the correlation. The elastic maps of the IDO-cuminaldehyde (Figure 4D), IDO-terpinen-7-al (Figure 5D), IDO-trans-anethole (Figure 6D), HMG-CoA-cuminaldehyde (Figure 7D), HMG-CoA-terpinen-7-al (Figure 8D), HMG-CoA-trans-anethole (Figure 9D), free IDO (Figure 10B), and free HMG-CoA (Figure 11B) proteins show the relationships between the atoms, with the stiffer parts indicated by the darker-gray areas. The mobility profiles of the docked proteins are provided by the B-factor and deformability. The deformability and B-factors of the IDO-cuminaldehyde (Figures 4E and 4F, respectively), IDO-terpinen-7-al (Figures 5E and 5F, respectively), IDO-trans-anethole (Figures 6E and 6F, respectively), HMG-CoA-cuminaldehyde (Figures 7E and 7F, respectively), HMG-CoA-terpinen-7-al (Figures 8E and 8F, respectively), HMG-CoA-trans-anethole (Figures 9E and 9F, respectively), free IDO (Figures 10C and 10D, respectively), and free HMG-CoA (Figures 11C and 11D, respectively) complexes depict the peaks that correspond to deformable areas in proteins, with the greatest peaks representing strong deformability. The eigenvalues and variance of the IDO-cuminaldehyde (Figures 4G and 4H, respectively), IDO-terpinen-7-al (Figures 5G and 5H, respectively), IDO-trans-anethole (Figures 6G and 6H, respectively), HMG-CoA-cuminaldehyde (Figures 7G and 7H, respectively), HMG-CoA-terpinen-7-al (Figures 8G and 8H, respectively), HMG-CoA-trans-anethole (Figures 9G and 9H, respectively), free IDO (Figures 10E and 10F, respectively), and free HMG-CoA (Figures 11E and 11F, respectively) complexes have an inverse relationship with each normal mode. The energy required to alter the structure is intimately related to the eigenvalues produced for the docked proteins. It represents the protein–ligand complex's stiffness of motion. The complex's deformability increases with decreasing eigenvalue [47]. The variance graph

uses purple-shaded bars to show individual variance and green-shaded bars to show cumulative variance. Based on the NMA, it was observed that every complex exhibited a substantial level of deformability of the bound proteins. Furthermore, all of the complexes exhibited low eigenvalues, suggesting that the molecular motions of the docked protein complexes were flexible and stable.

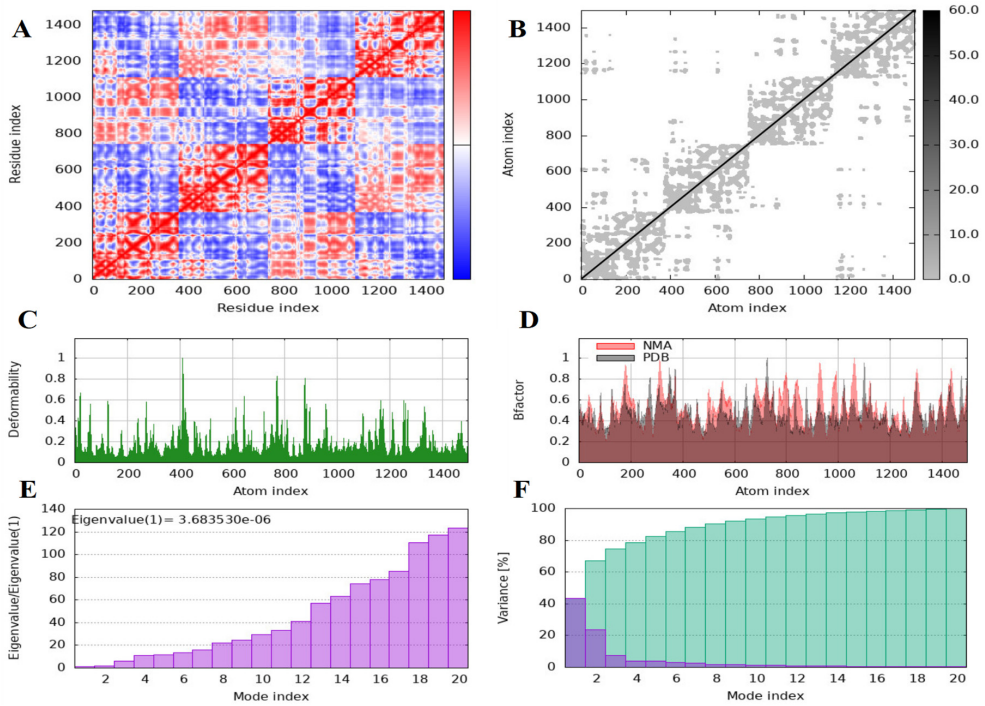


Figure 10. The normal mod analysis for IDO. (**A**) Elastic network model; (**B**) covariance map; (**C**) deformability; (**D**) B-factor plot; (**E**) eigenvalue plot; (**F**) variance plot.

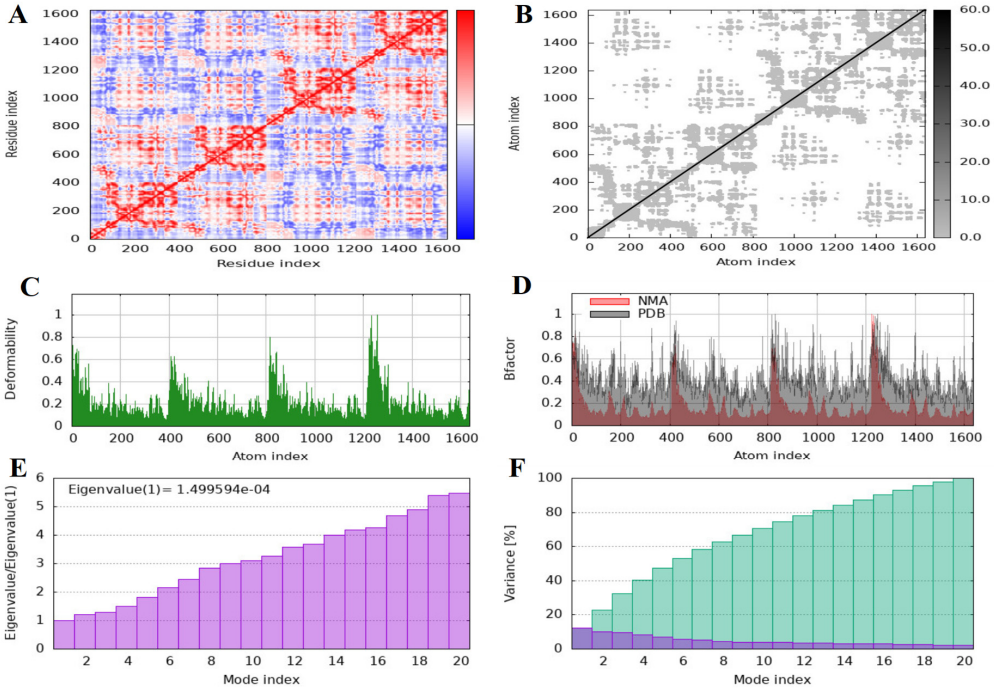


Figure 11. The normal mod analysis for HMG-CoA. (**A**) Elastic network model; (**B**) covariance map; (**C**) deformability; (**D**) B-factor plot; (**E**) eigenvalue plot; (**F**) variance plot.

3.3. The Particle Size, Polydispersity Index, and Zeta Potential of Cumin and Fennel EO Nanoparticles

According to Baranauskaite et al. [48], emulsion properties such as the z-average, zeta potential, and polydispersity index (PDI) have a direct relationship with encapsulation efficiency. Figure 12 shows the size distribution (A and B) and zeta potential (C and D) of the cumin and fennel EO nanocapsules, respectively. Table 4 summarizes the values of particle size (z-average hydrodynamic diameter), zeta potential, PDI, and EE% of the cumin and fennel EO nanoencapsules. Z-averages, PDI, and zeta potential are important indicators of emulsion physical stability during storage. The zeta potential describes the difference in electric potential between the particle's surface and the medium. Therefore, zeta potential values (negative or positive) near to 0 are related to unstable systems that sediment in a specific period [49]. The zeta potential plays a vital role in ensuring the physical stability of emulsions. A higher zeta potential, positive or negative, suggests increased emulsion stability. The zeta potential values of the cumin and fennel EO nanoemulsions indicated good colloidal stability. The PDI value represents the width of droplet size distribution and shows the homogeneity of generated nanodroplets in nanoemulsions. PDI values range from 0 to 1, with a closer to zero value indicating a more uniform distribution of particles [48]. Thus, the low PDI values of the cumin or fennel EO nanoemulsions indicate homogeneous distribution of the particles.

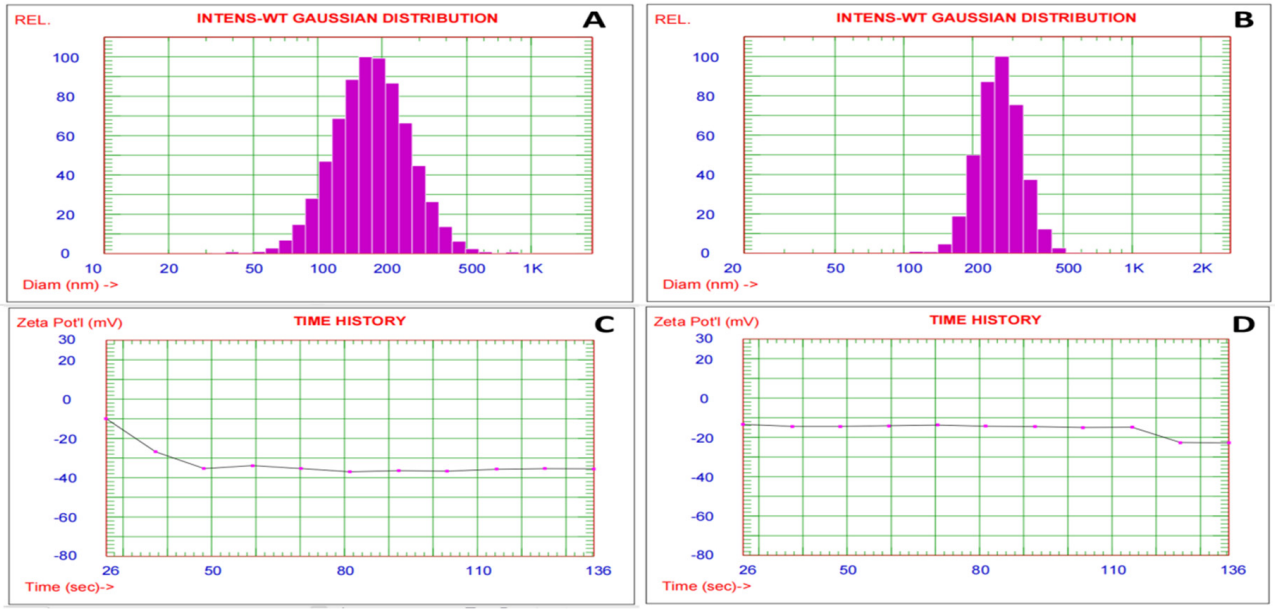


Figure 12. The size distribution of the cumin (**A**) and fennel (**B**) nanocapsules and the zeta potential of the cumin (**C**) and fennel (**D**) nanocapsules.

Table 4. Characteristics and antioxidant activity of cumin and fennel EO nanoparticles.

	CON	FON
Particle size (nm)	193.7 ± 77.30	269.3 ± 59.80
Zeta potential (mV)	−35.5 ± 2.34	−22.8 ± 1.55
PDI	0.159 ± 0.00	0.049 ± 0.00
EE (%)	89.36 ± 1.11	86.42 ± 0.94
DPPH (mg ascorbic acid equivalents/g nanocapsules)	68.36 ± 1.23	64.17 ± 1.35
FRAP (mg ascorbic acid equivalents/g nanocapsules)	57.23 ± 0.21	55.33 ± 0.17

3.4. In Vitro Antioxidant Activity of Cumin and Fennel EO Nanoparticles

According to the results (Table 4), the cumin and fennel EO nanocapsules demonstrated in vitro antioxidant activity via DPPH and FRAP assays. The antioxidant activity of natural products is mostly due to their ability to donate hydrogen, also known as radical scavenging. As hydrogen is transferred to DPPH, the color disappears. The greater the ability to transfer hydrogen, the stronger the bleaching impact [50]. The existence of aromatic rings, as well as the number and configuration of hydroxyl groups in EOs, may all contribute to the oil's antioxidant effects [51]. The retention of EOs within the nanostructure enables their dispersion in water, which improves their antioxidant action, as described by Jayari et al. [21]. An increase in free radicals is directly connected to a variety of health hazards, including reduced brain function. As a result, using natural products that are high in antioxidants will catch free radicals and minimize their detrimental impact on brain function [52]. The radical scavenging activity of cumin and fennel EO nanocapsules may contribute to the prevention of depression via inhibition of an increase in ROS, which stimulate oxidative stress in the brain, ultimately resulting in cellular demise and depression [6].

3.5. Release of the EO at Gastrointestinal pH

At 37 °C, the release behavior of fennel and cumin essential oils from the nanocapsules was assessed at several pH values, simulating the pH of intestinal (SIF; pH 6.5) and stomach (SGF; pH 2.5) fluids (Figure 13). Both oils showed a similar pattern. Rapid release (burst effect) from the nanocapsules was noted for the first half hour for both pH levels, which may have been caused by disruption of the nanocapsules in the presence of the fluid salts. The increased effect at pH 2.5 may be attributed to the fact that the hydrolysis of ester linkages in the acidic environment assisted the degradation of maltodextrin into acidic monomers, occurring through auto-catalytic mechanisms [53]. After this, a gradual growth rate was noted, with cumulative release values for cumin oil of 83% and 82%, and values for fennel oil of 84% and 82%, after 300 min in SGF and SIF conditions. *Citrus limon* essential oil microcapsules showed a similar pattern [31].

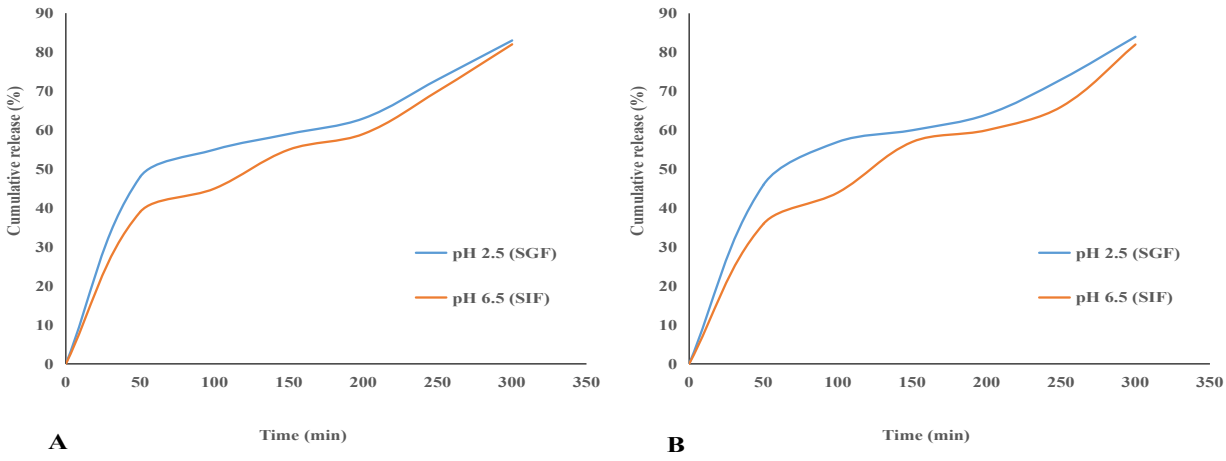


Figure 13. Release of the cumin (**A**) and fennel (**B**) EOs at gastrointestinal pH.

3.6. Scanning Electron Microscopy (SEM)

Using a scanning electron microscopy (SEM) assay, the size and shape of the freeze-dried cumin and fennel nanocapsules were observed. Figure 14 depicts cumin oil (A and B) and fennel oil (C and D) nanocapsules embedded in the structure of maltodextrin and Arabic gum polymers. The SEM images reveal that the EO nanocapsules have a round surface shape with a mean size of less than 200 nm.

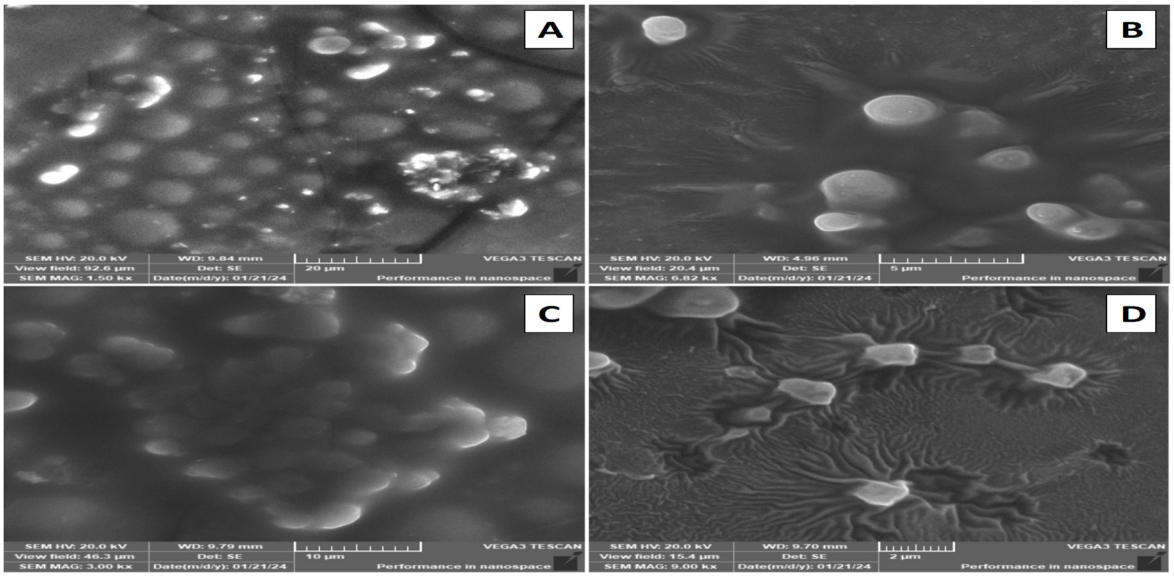


Figure 14. Scanning electron microscopy (SEM) images of the freeze-dried cumin and fennel EO nanocapsules. (**A**,**B**) SEM images of the cumin EO nanocapsules with magnifications of 1.5 and 6.8 kx, respectively. (**C**,**D**) SEM images of the fennel EO nanocapsules with magnifications of 3 and 9 kx, respectively.

3.7. In Vivo Study Findings

3.7.1. The Effect of Cumin and Fennel EO Nanoparticles on Sucrose Preference

The sucrose preference test was used to validate the presence of anhedonia, a key feature of depression. According to the sucrose preference results (Figure 15), the HFD/CMS group ingested considerably less sugar than the other groups ($p < 0.05$), indicating the presence of typical anhedonia, a hallmark of depression. These results are in line with those of Yang et al. [54], who found that obese rats exposed to CMS for three weeks had a lower sucrose preference percentage. Also, Parasuraman et al. [55] found that rats exposed to chronic unpredictable stress had a lower sucrose preference percentage. In contrast to the HFD/CMS group, the group treated with cumin and fennel EO nanocapsules had a significantly higher sucrose preference percentage ($p < 0.05$), indicating the capsules' antidepressant effect. The forced swim test (FST) and tail suspension test (TST), as additional depression indicators, were used by Asadi et al. [56] to confirm the antidepression-like effect of cumin EO. However, sucrose preference, as a dietary test, was more appropriate for our purposes.

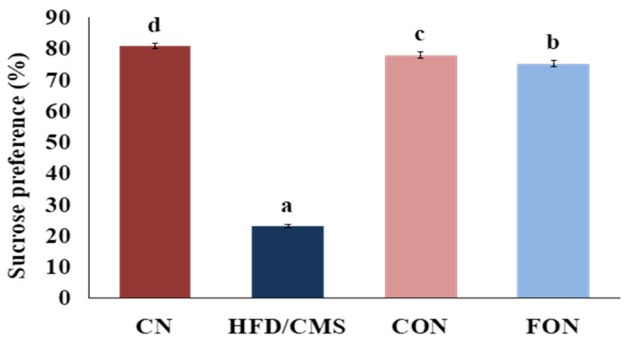


Figure 15. Percentage preference for sucrose in control normal (CN), HFD/CMS, cumin oil nanocapsule (CON), and fennel oil nanocapsule (FON) groups. The data are displayed as the mean ± SE ($n = 10$). The parts with different superscripts (a, b, c and d) are significantly different ($p < 0.05$). HFD/CMS, high-fat diet/chronic mild stress. a < b < c < d.

3.7.2. The Effect of Cumin and Fennel EO Nanoparticles on Growth Performance

Although the HFD/CMS group consumed less food, they gained significantly more body weight than the control group (Table 5). These findings are consistent with those revealed in the study by Lippi [33], which found that HFD/CMD-treated mice ate less and weighed substantially more than normal mice. Treatment with cumin and fennel EO nanocapsules resulted in a significant trend of reduced body weight gain when compared to the HFD/CMS group, which could be attributed to moderate effects of reduced lipid formation in adipocytes. Jafari et al. [14] found that pre-diabetic participants lost weight and had a smaller waist circumference after consuming 75 mg of cumin oil per day. Haque and Ansari [57] reported that cuminaldehyde prevented weight gain in high-fat fed rats by lowering the visceral fat pat weight. As reported by Kang et al. [58], beige adipocyte-specific genes were expressed when mice were treated with trans-anethole. Additionally, by boosting mitochondrial biogenesis in white adipocytes and stimulating brown adipocytes, trans-anethole demonstrated thermogenic activity. The trials also demonstrated that trans-anethole enhanced lipolysis and fat oxidation while decreasing adipogenesis and lipogenesis. Kang et al. [58] also discovered that trans-anethole activated sirtuin1 (SIRT1) and the β3-adrenergic receptor to cause browning in 3T3-L1 adipocytes. SIRT1 stimulated the expression of proteins (UCP1, PRDM16, PGC-1a, AMPK, and pAMPK) involved in lipid metabolism.

Table 5. The growth performance of the control normal (CN), HFD/CMS, cumin oil nanocapsule (CON), and fennel oil nanocapsule (FON) groups.

	CN	HFD/CMS	CON	FON
Initial body weight (g)	$35.40^{a} \pm 0.72$	$35.10^{a} \pm 0.92$	$35.40^{a} \pm 1.14$	$35.10^{a} \pm 0.91$
Final body weight (g)	$69.20^{a} \pm 1.47$	$76.80^{b} \pm 1.73$	$69.60^{a} \pm 1.13$	$71.40^{a} \pm 1.49$
Body weight gain (g)	$33.80^{a} \pm 0.93$	$41.70^{b} \pm 1.05$	$34.20^{a} \pm 0.70$	$36.30^{a} \pm 0.84$
Daily food intake (g)	13.94	13.23	13.56	13.47

Data are displayed as mean ± SE (n = 10). Different superscripts (a and b) in each row indicate significant differences ($p < 0.05$). HFD/CMS, high-fat diet/chronic mild stress. a < b.

3.7.3. The Effect of Cumin and Fennel EO Nanoparticles on Neurotransmitters and Inflammatory Markers in the Brain

Measurements of pro-inflammatory TLR4, TNF-α, and IL-6 can be used to quantify inflammation. Our results (Figure 16) show that the HFD/CMS group had significantly ($p < 0.05$) lower levels of serotonin and dopamine than the CN group, indicating anxiety and depression. On the other hand, the HFD/CMS group exhibited significant ($p < 0.05$) increase levels of AChE, TLR4, TNF-α, and IL-6 in comparison to the CN group. Abbasi-Maleki and Maleki [59] proposed that fennel EO has an antidepressant effect via stimulating the dopaminergic and serotonergic neural systems, and they discovered that fennel EO-treated mice swam longer in the forced swim test than normal mice. Furthermore, earlier research has demonstrated that the major ingredient of fennel EO, anethole, produces antidepressive-like effects in animal models via various pathways [60,61]. The present results are consistent with other studies [62] that have shown elevated levels of AChE, TNF-α, and CRP in rats fed a high-fat diet. According to Felger et al. [63], patients with major depression had lower concentrations of IL-10 and higher concentrations of inflammatory cytokines (TNF-α, IL-1β, IL-6, and CRP) when compared to healthy controls. These findings suggest that inflammation plays a critical role in the pathophysiology of depression. According to Gao et al. [2], increased inflammatory damage is the mechanism via which HFD/CUMS causes behavior resembling depression. TLR4 activation is linked to the inflammatory response, which modifies the structure and function of the tissues in the brain and small intestine. Therefore, medications that inhibit TLR4 activation may help to lessen the symptoms

associated with depression. Additionally, cuminaldehyde and trans-anethole may help to reduce stress-induced behavioral and psychological disorders by altering the structure of the gut microbiota through the microbiota–gut–brain axis [64,65].

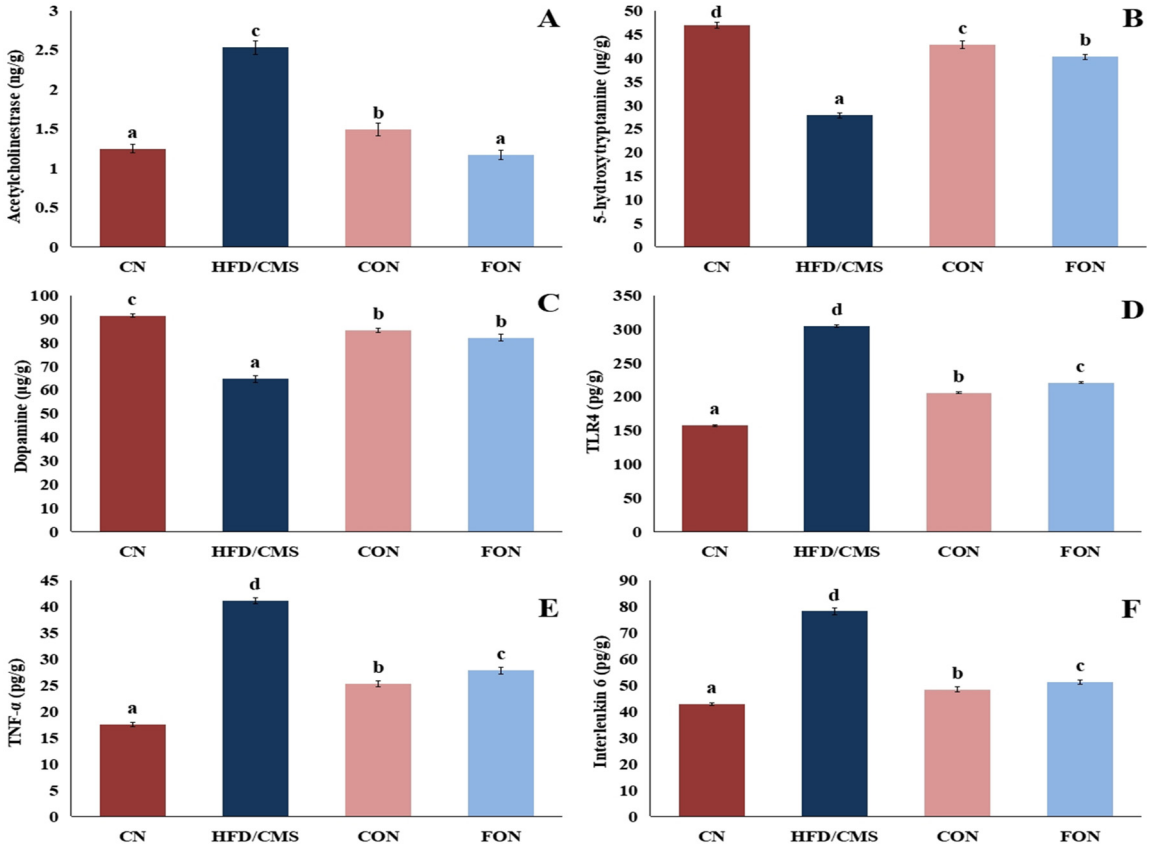


Figure 16. Neurotransmitters and inflammatory cytokines in the control normal (CN), HFD/CMS, cumin oil nanocapsule (CON), and fennel oil nanocapsule (FON) groups. The data are displayed as the mean ± SE (n = 10). The parts with different superscripts (a, b, c and d) are significantly different ($p < 0.05$). HFD/CMS, high-fat diet/chronic mild stress. (**A**) acetylcholinesterase; (**B**) 5-hydroxytryptamine; (**C**) dopamine; (**D**) TLR4; (**E**) TNF-α; (**F**) IL-6. a < b < c < d.

In this investigation, the CON and FON groups had significantly ($p < 0.05$) higher levels of 5-HT and dopamine than the HFD/CMS group. Conversely, the CON and FON groups had significantly ($p < 0.05$) lower levels of AChE, TLR4, TNF-α, and IL-6 than the HFD/CMS group. Mice treated with cumin EO nanocapsules had significantly ($p < 0.05$) higher levels of AChE, TLR4, TNF-α, and IL-6 than mice treated with fennel EO nanocapsules. Fennel and cumin essential oils have an anti-inflammatory action that may help to prevent depression. Wei et al. [13] proposed that cumin oil inhibited the signaling of mitogen-activated protein kinases and NF-κB to produce anti-inflammatory effects. The constituents of cumin and fennel EOs may be responsible for their anti-inflammatory properties. Cuminaldehyde has been discovered to have an anti-inflammatory impact and reduce pro-inflammatory cytokines in rat models [66]. Yu et al. [67] declared that trans-anethole has been demonstrated to exert an anti-inflammatory impact in many types of inflammatory disorders and reduces activation of the TLR4/NF-κB signaling pathway.

3.7.4. The Effect of Cumin and Fennel EO Nanoparticles on Oxidant and Antioxidant Markers in the Brain

Measurements of oxidative stress biomarkers such MDA, SOD, CAT, and GSH can be used to quantify oxidative stress in the brain. As seen in our results (Figure 17), the

HFD/CMS group's mice showed significantly lower levels of GSH, CAT, and SOD, and significantly higher levels of ROS, NO, and MDA, when compared to the normal mice. After feeding rats on a high-fat diet, Azmi et al. [62] observed similar outcomes. Conversely, in contrast to the HFD/CMS group, the administration of cumin and fennel EOs, and particularly cumin nanocapsules, afforded antioxidant activity, as evidenced by a decrease in ROS, NO, and MDA values and an increase in GSH, CAT, and SOD values. The constituents of fennel and cumin EOs may be responsible for their antioxidant properties. A study by Chen et al. [68] demonstrated that cumin oil has an excellent capacity to reduce lipid peroxidation and exhibits better antioxidant activity than BHT. Chen et al. [68] found that the potent antioxidant present in cumin oil was γ-terpinene. Anethole, the quantitatively dominant component in fennel essential oil, is thought to be responsible for the antioxidant and anti-inflammatory properties of fennel. As stated by Mohamed et al. [69], anethole possesses anti-inflammatory and anti-apoptotic properties, which are demonstrated by elevated GSH and CAT levels and decreased levels of MDA, TNF-alpha, interferon-gamma, and interleukin 10.

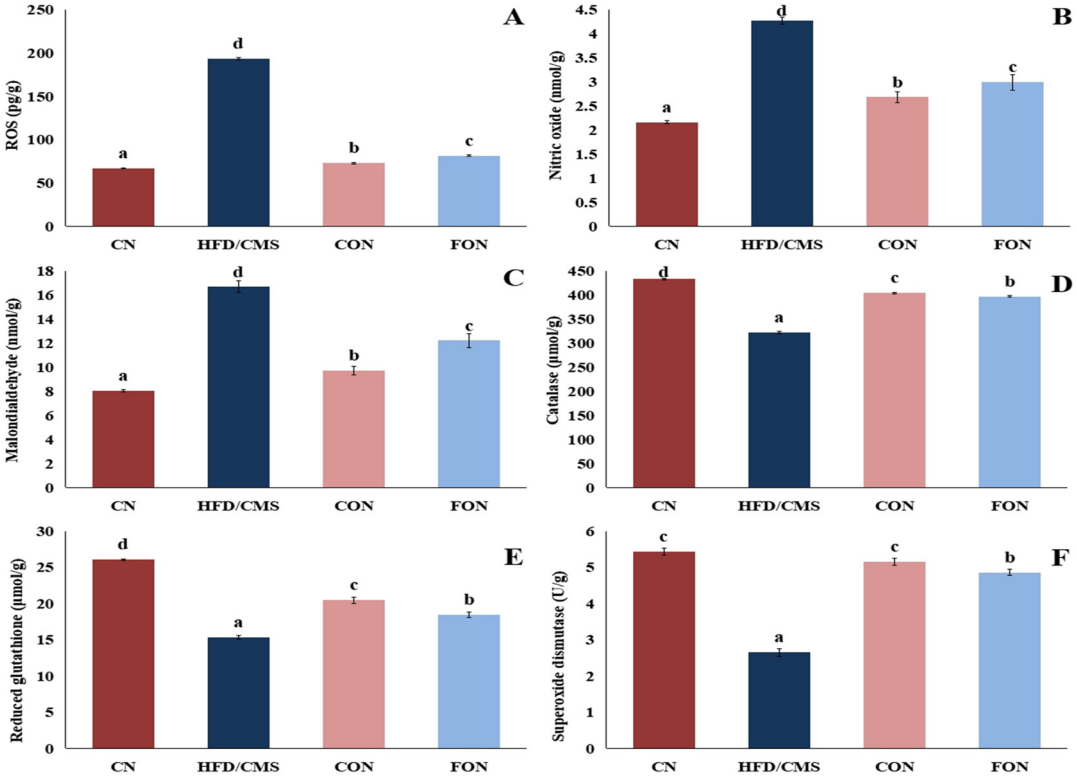


Figure 17. Oxidant and antioxidant markers in the control normal (CN), HFD/CMS, cumin oil nanocapsule (CON), and fennel oil nanocapsule (FON) groups. The data are displayed as the mean ± SE (n = 10). The parts with different superscripts (a, b, c and d) are significantly different ($p < 0.05$). HFD/CMS, high-fat diet/chronic mild stress. (**A**) ROS; (**B**) nitric oxide; (**C**) MDA; (**D**) CAT; (**E**) GSH; (**F**) SOD. a < b < c < d.

3.7.5. The Effect of Cumin and Fennel EO Nanoparticles on the Lipid Profile

It has been observed that when dyslipidemia and depression coexist, both of them may cause acute anxiety symptoms [70]. Our results (Figure 18) show that in comparison to the normal mice, the HFD/CMS group's mice had significantly higher levels of cholesterol, TGs, LDL, non-HDL cholesterol, and VLDL, and a higher Ch/HDL ratio, while the HDL value was significantly lower. These findings concur with those reported by Wang et al. [71], who observed elevated levels of TGs, LDL, and cholesterol in rats given a high-fat diet and subjected to CMS. As confirmed by Azmi et al. [62], feeding on an HFD is involved in this

change in lipid profile that leads to dyslipidemia. Depression has been linked to blood levels of total cholesterol, low-density lipoprotein cholesterol, triglycerides, and high-density lipoprotein cholesterol, in accordance with studies by Jia et al. [72] and Han [73]. In the study by Lin et al. [74], rats subjected to mild stress demonstrated antidepressant-like responses to lipid-lowering agents. It is interesting to note that as compared to the HFD/CMS group, the CON and FON groups, particularly the CON group, showed significantly ($p < 0.05$) lower levels of cholesterol, TGs, LDL, non-HDL cholesterol, and VLDL, along with a lower Ch/HDL ratio and higher levels of HDL. A study conducted by Jafari et al. [14] found that the consumption of 75 mg/d of cumin oil improved the pre-diabetic participants' lipid profile parameters, and the researchers reported that cuminaldehyde is responsible for stimulating LDL-C receptors, leading the removal of LDL-C from the bloodstream and a decrease in the production of oxidized LDL. Also, Hong et al. [18] found that fennel EO suppressed lipid and metabolic abnormalities in rats fed a high-fat diet. The hypolipidemic effects of cumin and fennel EOs may be attributed to their constituents, as explained by Haque and Ansari [57], who found that cuminaldehyde reduced cholesterol, TGs, and LDL while increasing HDL in rats fed a high-fat diet. Similarly, Samadi-Noshahr et al. [75] reported that trans-Anethole decreased the levels of cholesterol, TGs, and LDL in diabetic rats.

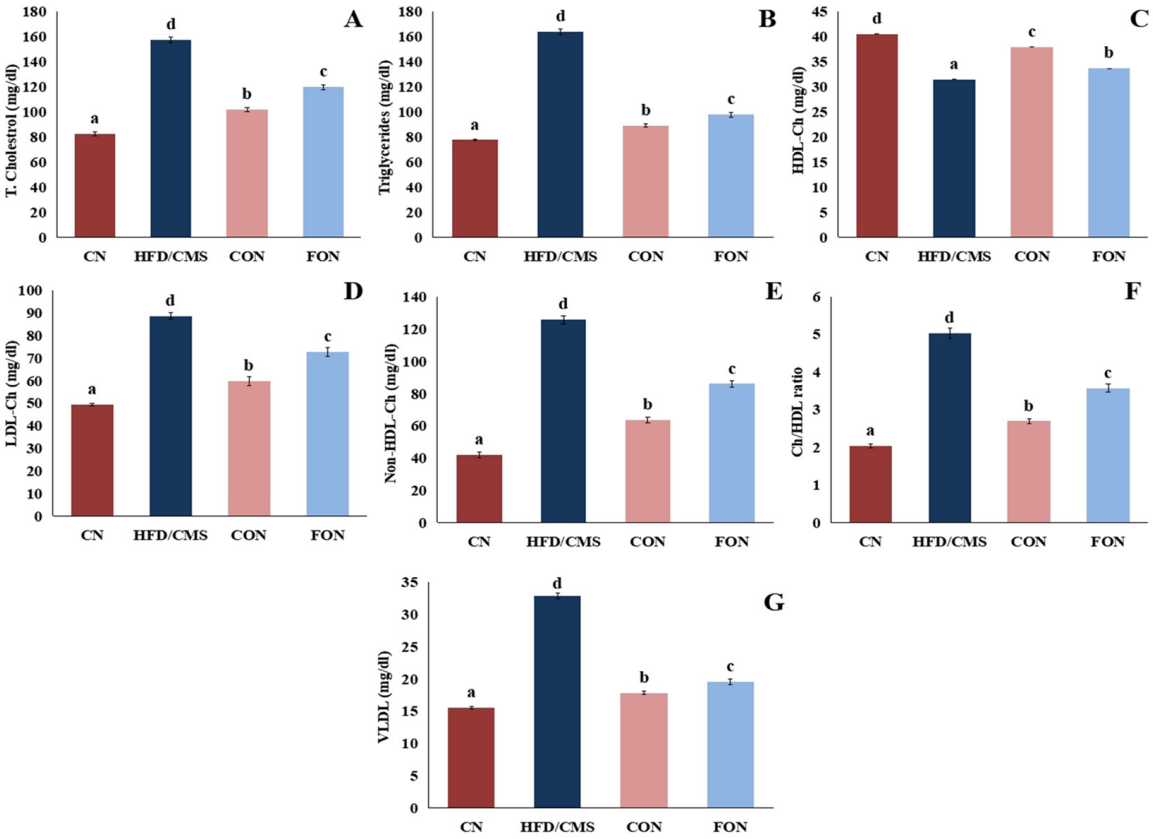


Figure 18. The lipid profiles of the control normal (CN), HFD/CMS, cumin oil nanocapsule (CON), and fennel oil nanocapsule (FON) groups. The data are displayed as the mean ± SE ($n = 10$). The parts with different superscripts (a, b, c and d) are significantly different ($p < 0.05$). HFD/CMS, high-fat diet/chronic mild stress. (**A**) Total cholesterol; (**B**) triglycerides; (**C**) HDL-Ch; (**D**) LDL-Ch; (**E**) non-HDL-Ch; (**F**) Ch/HDL ratio; (**G**) VLDL. a < b < c < d.

3.7.6. The Effect of Cumin and Fennel EO Nanoparticles on Liver and Kidney Function

Liver function and kidney function were assessed to examine the effect of cumin and fennel nanocapsules on the liver and kidneys, as well as the effectiveness of these

nanocapsules in protecting the liver and kidneys from free radicals and inflammatory cytokines, which increase not only with high-fat diet consumption, but also as a result of chronic stress exposure. According to the findings (Table 6), mice in the HFD/CMS group had significantly higher values for AST, ALT, ALP, urea, creatinine, LDH, and albumin than normal mice. Wang et al. [71] disclosed that rats given an HFD and exposed to CMS had elevated levels of ALP, globulin, and albumin. Interestingly, the antioxidant and anti-inflammatory actions of cumin and fennel EOs helped to restore liver and function in the CON and FON groups, which had significantly lower AST, ALT, ALP, urea, creatinin, LDH, and albumin levels than the HFD/CMS group. Haque and Ansari [57] reported that cuminaldehyde reduced AST and ALT in rats fed a high-fat diet.

Table 6. Liver and kidney function of control normal (CN), HFD/CMS, cumin oil nanocapsule (CON), and fennel oil nanocapsule (FON) groups.

	CN	HFD/CMS	CON	FON
AST (U/L)	$46.78^{b} \pm 0.61$	$73.20^{c} \pm 1.41$	$48.70^{b} \pm 1.11$	$42.00^{a} \pm 0.75$
ALT (U/L)	$27.66^{a} \pm 0.41$	$63.80^{c} \pm 1.07$	$36.90^{b} \pm 0.94$	$38.30^{b} \pm 1.03$
LDH (U/L)	$240.80^{a} \pm 0.85$	$381.70^{d} \pm 1.58$	$259.00^{b} \pm 1.32$	$278.90^{c} \pm 1.75$
Urea (mg/dL)	$26.50^{a} \pm 0.34$	$37.20^{d} \pm 0.49$	$29.50^{b} \pm 0.69$	$33.20^{c} \pm 0.83$
Creatinine (mg/dL)	$0.35^{a} \pm 0.01$	$0.81^{c} \pm 0.02$	$0.47^{b} \pm 0.02$	$0.51^{b} \pm 0.02$
Albumin (g/dL)	$4.26^{d} \pm 0.06$	$2.18^{a} \pm 0.05$	$4.01^{c} \pm 0.07$	$3.70^{b} \pm 0.10$
ALP (U/L)	$125.90^{a} \pm 0.78$	$159.10^{d} \pm 1.69$	$130.70^{b} \pm 0.75$	$143.20^{c} \pm 1.25$

Data are displayed as mean ± SE (n = 10). Different superscripts (a, b, c and d) in each row indicate significant differences ($p < 0.05$). HFD/CMS, high-fat diet/chronic mild stress. a < b < c < d.

4. Conclusions

Cuminaldehyde, γ-terpinen-7-al, α-terpinen-7-al, γ-terpinene, and p-cymene are the primary constituents of cumin EO, while trans-anethole, D-limonene, and L-fenchone are the primary constituents of fennel EO. In silico molecular docking revealed that terpinen-7-al exhibited the highest binding affinity for the IDO and HMG-CoA receptors, and also interacted with their active sites through both hydrophobic interactions and hydrogen bonds. Trans-anethole strongly interacted with the active sites of the HMG-CoA receptor via both hydrophobic interactions and a hydrogen bond. The cumin and fennel nanocapsules showed in vitro antioxidant activity. The in vivo findings demonstrated that an HFD combined with CMS exposure caused a depression-like state, as evidenced by a decrease in sucrose preference and changes in brain dopamine and serotonin levels. HFD and CMS elevated inflammatory and oxidative markers in the brain, while reducing antioxidant enzyme activity. In contrast, the cumin and fennel EO nanocapsules showed protective efficacy against a depression-like state. The cumin and fennel EO nanocapsules lowered the levels of inflammatory cytokines (TLR4, TNF-α, and IL-6) and oxidant markers (ROS, MDA, and NO) in the brain, while enhancing sucrose preference, dopamine levels, serotonin levels, and antioxidant enzyme activity (GSH, SOD, and CAT). The cumin and fennel EO nanocapsules lowered cholesterol, TG, and LDL-ch levels. The cumin EO nanocapsules showed more promise for improvement. The results reveal the potential hypolipidemic and antidepressant effects of cumin and fennel EO nanocapsules. Further studies on humans are required. Also, future studies on the effect of cumin and fennel nanocapsules on gut microbiome dysbiosis induced by high-fat diets may be useful in further explaining the mechanism of action of these nanocapsules.

Author Contributions: K.F.: Writing—Review and Editing, Methodology, Investigation, Formal Analysis. R.S.M.: Writing—Original Draft, Methodology, Investigation, Formal Analysis, Conceptualization. All authors have read and agreed to the published version of the manuscript.

Funding: This research received no external funding.

Institutional Review Board Statement: All experiments were carried out according to research protocols approved by the Medical Research Ethics Committee (MREC) at the National Research Centre, which are in accordance with the provisions of the relevant Egyptian laws and with Helsinki Declaration, as well as the institutional Animal Care and Use Committee (IACUC) guidelines and recommendations and WHO rules regarding the ethics of scientific research. Ethical Approval Certificate No. 180572022. The approval date: 4 December 2022.

Data Availability Statement: Data will be made available on request.

Acknowledgments: The authors are thankful for the technical support of the National Research Centre, Egypt.

Conflicts of Interest: The authors declare that they have no known competing financial interest or personal relationships that could appear to have influenced the work reported in this paper.

References

1. Francis, H.M.; Stevenson, R.J.; Tan, L.S.Y.; Ehrenfeld, L.; Byeon, S.; Attuquayefio, T.; Gupta, D.; Lim, C.K. Kynurenic acid as a biochemical factor underlying the association between Western-style diet and depression: A cross-sectional study. *Front. Nutr.* **2022**, *9*, 945538. [CrossRef]
2. Gao, L.N.; Yan, M.; Zhou, L.; Wang, J.; Sai, C.; Fu, Y.; Liu, Y.; Ding, L. Puerarin Alleviates Depression-Like Behavior Induced by High-Fat Diet Combined with Chronic Unpredictable Mild Stress via Repairing TLR4- Induced Inflammatory Damages and Phospholipid Metabolism Disorders. *Front. Pharmacol.* **2021**, *12*, 767333. [CrossRef]
3. Cervellati, C.; Trentini, A.; Pecorelli, A.; Valacchi, G. Inflammation in Neurological Disorders: The Thin Boundary between Brain and Periphery. *Antioxid. Redox Signal.* **2020**, *33*, 191–210. [CrossRef] [PubMed]
4. Lützhøft, D.O.; Bækgård, C.; Wimborne, E.; Straarup, E.M.; Pedersen, K.M.; Swann, J.R.; Pedersen, H.D.; Kristensen, K.; Morgills, L.; Nielsen, D.S.; et al. High fat diet is associated with gut microbiota dysbiosis and decreased gut microbial derived metabolites related to metabolic health in young Göttingen Minipigs. *PLoS ONE* **2024**, *19*, e0298602. [CrossRef] [PubMed]
5. Wang, Q.; Jia, M.; Zhao, Y.; Hui, Y.; Pan, J.; Yu, H.; Yan, S.; Dai, X.; Liu, X.; Liu, Z. Supplementation of sesamin alleviates stress-induced behavioral and psychological disorders via reshaping the gut microbiota structure. *J. Agric. Food Chem.* **2019**, *67*, 12441–12451. [CrossRef] [PubMed]
6. Lu, X.; Qi, C.; Zheng, J.; Sun, M.; Jin, L.; Sun, J. The Antidepressant Effect of Deoiled Sunflower Seeds on Chronic Unpredictable Mild Stress in Mice Through Regulation of Microbiota–Gut–Brain Axis. *Front. Nutr.* **2022**, *9*, 908297. [CrossRef]
7. Korinek, M.; Handoussa, H.; Tsai, Y.H.; Chen, Y.Y.; Chen, M.H.; Chiou, Z.W.; Fang, Y.; Chang, F.R.; Yen, C.H.; Hsieh, C.F.; et al. Anti-Inflammatory and Antimicrobial Volatile Oils: Fennel and Cumin Inhibit Neutrophilic Inflammation via Regulating Calcium and MAPKs. *Front. Pharmacol.* **2021**, *12*, 674095. [CrossRef]
8. Tang, D.; Liang, Q.; Zhang, M.; Li, M.; Zhang, Q.; Zhang, S.; Ai, L.; Wu, C. Anti-depression effectiveness of essential oil from the fruits of *Zanthoxylum bungeanum* maxim. on chronic unpredictable mild stress-induced depression behavior in mice. *Front. Pharmacol.* **2022**, *13*, 999962. [CrossRef]
9. Fonseca, E.C.; Ferreira, L.R.; Figueiredo, P.L.; Maia, C.D.; Setzer, W.N.; Da Silva, J.K. Antidepressant Effects of Essential Oils: A Review of the Past Decade (2012–2022) and Molecular Docking Study of Their Major Chemical Components. *Int. J. Mol. Sci.* **2022**, *24*, 9244. [CrossRef]
10. Zhao, Y.; Wang, P.; Zheng, W.; Yu, G.; Li, Z.; She, Y.; Lee, M. Three-stage microwave extraction of cumin (*Cuminum cyminum* L.) Seed essential oil with natural deep eutectic solvents. *Ind. Crops Prod.* **2019**, *140*, 111660. [CrossRef]
11. Iram, N.; Edwin, E.C. Chemical composition, essential oil characterization and antibacterial activity of cumin (*Cuminum cyminum*). *Pak. Biomed. J.* **2022**, *5*, 86–90. [CrossRef]
12. Nikkhah, A.; Nikkhah, H.; Shahbazi, A.; Zarin, M.K.Z.; Beykal, I.D.; Ebadi, M.T.; Fakhroleslam, M.; Beykal, B. Cumin and eucalyptus essential oil standardization using fractional distillation: Data-driven optimization and techno-economic analysis. *Food Bioprod. Process.* **2024**, *143*, 90–101. [CrossRef]
13. Wei, J.; Zhang, X.; Bi, Y.; Miao, R.; Zhang, Z.; Su, H. Anti-Inflammatory Effects of Cumin Essential Oil by Blocking JNK, ERK, and NF-κB Signaling Pathways in LPS-Stimulated RAW 264.7 Cells. *Evid. Based Complement. Altern. Med.* **2015**, *2015*, 474509. [CrossRef] [PubMed]
14. Jafari, T.; Mahmoodnia, L.; Tahmasebi, P.; Memarzadeh, M.R.; Sedehi, M.; Beigi, M.; Fallah, A.A. Effect of cumin (*Cuminum cyminum*) essential oil supplementation on metabolic profile and serum leptin in pre-diabetic subjects: A randomized double-blind placebo-controlled clinical trial. *J. Funct. Foods* **2018**, *47*, 416–422. [CrossRef]

15. Haque, M.R.; Ansari, S.H. Aromatic aldehyde compound cuminaldehyde protects nonalcoholic fatty liver disease in rats feeding high fat diet. *Hum. Exp. Toxicol.* **2019**, *38*, 823–832. [CrossRef] [PubMed]
16. Imbabi, T.; Sabeq, I.; Osman, A.; Mahmoud, K.; Amer, S.A.; Hassan, A.M.; Kostomakhin, N.; Habashy, W.; Easa, A.A. Impact of Fennel Essential Oil as an Antibiotic Alternative in Rabbit Diet on Antioxidant Enzymes Levels, Growth Performance, and Meat Quality. *Antioxidants* **2021**, *10*, 1797. [CrossRef]
17. Barakat, H.; Alkabeer, I.A.; Althwab, S.A.; Alfheeaid, H.A.; Alhomaid, R.M.; Almujaydil, M.S.; Almuziree, R.S.A.; Bushnaq, T.; Mohamed, A. Nephroprotective Effect of Fennel (*Foeniculum vulgare*) Seeds and Their Sprouts on CCl4-Induced Nephrotoxicity and Oxidative Stress in Rats. *Antioxidants* **2023**, *12*, 325. [CrossRef]
18. Hong, S.J.; Yoon, S.; Jo, S.M.; Jeong, H.; Youn, M.Y.; Kim, Y.J.; Kim, J.K.; Shin, E.C. Olfactory Stimulation by Fennel (*Foeniculum vulgare* Mill.) Essential Oil Improves Lipid Metabolism and Metabolic Disorders in High Fat-Induced Obese Rats. *Nutrients* **2022**, *14*, 741. [CrossRef]
19. Neetu, J.S.; Sunil, K.; Rana, A.C. Antidepressant activity of methanolic extract of *Foeniculum vulgare* (Fennel) fruits in experimental animal models. *Int. J. Pharm. Sci. Res.* **2013**, *3*, 065–070. [CrossRef]
20. Singh, S.P. A comprehensive review on pharmacological activity of *Foeniculum vulgare*. *Glob. J. Pharm. Sci.* **2019**, *7*, 23–27. [CrossRef]
21. Jayari, A.; Donsì, F.; Ferrari, G.; Maaroufi, A. Nanoencapsulation of Thyme Essential Oils: Formulation, Characterization, Storage Stability, and Biological Activity. *Foods* **2022**, *11*, 1858. [CrossRef]
22. Luo, S.; Xu, K.; Xiang, S.; Chen, J.; Chen, C.; Guo, C.; Tong, Y.; Tong, L. High-resolution structures of inhibitor complexes of human indoleamine 2,3-dioxygenase 1 in a new crystal form. *Acta Crystallogr. F Struct. Biol. Commun.* **2018**, *74*, 717–724. [CrossRef]
23. Gesto, D.S.; Pereira, C.M.S.; Cerqueira, N.M.F.S.; Sousa, S.F. An Atomic-Level Perspective of HMG-CoA-Reductase: The Target Enzyme to Treat Hypercholesterolemia. *Molecules* **2020**, *25*, 3891. [CrossRef] [PubMed]
24. Othman, I.M.; Mahross, M.H.; Gad-Elkareem, M.A.; Rudrapal, M.; Gogoi, N.; Chetia, D.; Aouadi, K.; Snoussi, M.; Kadri, A. Toward a treatment of antibacterial and antifungal infections: Design, synthesis and in vitro activity of novel arylhydrazothiazolylsulfonamides analogues and their insight of DFT, docking and molecular dynamic simulations. *J. Mol. Struct.* **2021**, *1243*, 130862. [CrossRef]
25. Trott, O.; Olson, A.J. AutoDock Vina: Improving the speed and accuracy of docking with a new scoring function, efficient optimization, and multithreading. *J. Comput. Chem.* **2010**, *31*, 455–461. [CrossRef] [PubMed]
26. López-Blanco, J.R.; Aliaga, J.I.; Quintana-Ortí, E.S.; Chacón, P. iMODS: Internal coordinates normal mode analysis server. *Nucleic Acids Res.* **2014**, *42*, W271–W276. [CrossRef]
27. Mahdi, A.A.; Al-Maqtari, Q.A.; Mohammed, J.K.; Al-Ansi, W.; Aqeel, S.M.; Cui, H.; Lin, L. Nanoencapsulation of Mandarin Essential Oil: Fabrication, Characterization, and Storage Stability. *Foods* **2021**, *11*, 54. [CrossRef]
28. Pudžiuvelytė, L.; Petrauskaitė, E.; Stabrauskienė, J.; Bernatonienė, J. Spray-Drying Microencapsulation of Natural Bioactives: Advances in Sustainable Wall Materials. *Pharmaceuticals* **2025**, *18*, 963. [CrossRef]
29. Dwivedy, A.K.; Singh, V.K.; Prakash, B.; Dubey, N.K. Nanoencapsulated *Illicium verum* Hook.f. essential oil as an effective novel plant-based preservative against aflatoxin B1 production and free radical generation. *Food Chem. Toxicol.* **2018**, *111*, 102–113. [CrossRef]
30. Asres, Y.; Hymete, A.; Admassu, H.; Ayalew, A. Application of microencapsulated essential oil extracted from Thymus schimperi for its antibacterial and antioxidant activity on minced meat. *Discov. Appl. Sci.* **2025**, *7*, 485. [CrossRef]
31. Djihad, N.; Naima, F.O.; Petronilho, S.; Hamid, S.; Bedjou, F.N.E.; Coimbra, M.A. Microencapsulation of Citrus limon essential oil by complex coacervation and release behavior of terpenic and derived volatile compounds. *Food Hydrocoll.* **2024**, *152*, 109830. [CrossRef]
32. Mohamed, R.S.; Fouda, K.; Zaghloul, A.H.; Abdel-Salam, A.M. Potential antidiabetic activity of probiotic and Garcinia kola-yoghurt and its role in regulation of male fertility-stimulating hormones in high-fat diet/low dose streptozotocin-treated rats. *Food Prod. Process. Nutr.* **2024**, *6*, 55. [CrossRef]
33. Lippi, S.L.P. Chronic Mild Unpredictable Stress and High-Fat Diet Given during Adolescence Impact Both Cognitive and Noncognitive Behaviors in Young Adult Mice. *Brain Sci.* **2021**, *11*, 260. [CrossRef]
34. Moubarz, G.; Embaby, M.A.; Doleib, N.M.; Taha, M.M. Effect of dietary antioxidant supplementation (*Cuminum cyminum*) on bacterial susceptibility of diabetes-induced rats. *Cent. Eur. J.* **2016**, *2*, 123–137. [CrossRef] [PubMed]
35. Asaad, G.F.; Redai, A.Q.; Hakami, A.O.; Ghazwani, F.Y.; Nomier, Y.; Alshahrani, S. Potential analgesic and anti-inflammatory effect of *Cuminum cyminum* and *Borago officinalis* in rats and mice. *Asian J. Pharm. Clin. Res.* **2020**, *13*, 216–218. [CrossRef]
36. Liu, M.Y.; Yin, C.Y.; Zhu, L.J.; Zhu, X.H.; Xu, C.; Luo, C.X.; Chen, H.; Zhu, D.Y.; Zhou, Q.G. Sucrose preference test for measurement of stresss-induced anhedonia in mice. *Nat. Protoc.* **2018**, *13*, 1686–1698. [CrossRef] [PubMed]
37. Mohamed, A.S.; Hosney, M.; Bassiony, H.; Hassanein, S.S.; Soliman, A.M.; Fahmy, S.R.; Gaafar, K. Sodium pentobarbital dosages for exsanguination affect biochemical, molecular and histological measurements in rats. *Sci. Rep.* **2020**, *10*, 378. [CrossRef]

38. Mohamed, R.S.; Fouda, K.; Salama, A.; Akl, E.M. Peanut meal-derived bioactive compounds: Extraction, co-extrusion encapsulation and neuroprotection against aluminum-induced Alzheimer's disease via in silico and in vivo studies. *Phytomed. Plus* **2024**, *4*, 100588. [CrossRef]
39. Moradi, A.; Davati, N.; Emamifar, A. Effects of *Cuminum cyminum* L. essential oil and its nanoemulsion on oxidative stability and microbial growth in mayonnaise during storage. *Food Sci. Nutr.* **2023**, *11*, 4781–4793. [CrossRef]
40. Stefănescu, R.; Osz, B.E.; Pintea, A.; Laczkó-Zöld, E.; Tero-Vescan, A.; Vari, C.E.; Fulop, E.; Blas, I.; Vancea, S. Fennel Essential Oil as a Complementary Therapy in the Management of Diabetes. *Pharmaceutics* **2023**, *15*, 2657. [CrossRef]
41. Saleem, U.; Shehzad, A.; Shah, S.; Raza, Z.; Shah, M.A.; Bibi, S.; Chauhdary, Z.; Ahmad, B. Antiparkinsonian activity of Cucurbita pepo seeds along with possible underlying mechanism. *Metab. Brain Dis.* **2021**, *36*, 1231–1251. [CrossRef]
42. de Oliveira, J.; Engel, D.F.; de Paula, G.C.; dos Santos, D.B.; Lopes, J.B.; Farina, M.; Moreira, E.L.G.; de Bem, A.F. High Cholesterol Diet Exacerbates Blood-Brain Barrier Disruption in LDLr−/− Mice: Impact on Cognitive Function. *J. Alzheimer's Dis.* **2020**, *78*, 97–115. [CrossRef]
43. Qin, Y.; Wang, N.; Zhang, X.; Han, X.; Zhai, X.; Lu, Y. IDO and TDO as a potential therapeutic target in different types of depression. *Metab. Brain Dis.* **2018**, *33*, 1787–1800. [CrossRef]
44. Shah, M.A.; Muhammad, H.; Mehmood, Y.; Khalil, R.; Ul-Haq, Z.; Panichayupakaranant, P. Superoxide Scavenging and Antiglycation Activity of Rhinacanthins-rich Extract Obtained from the Leaves of Rhinacanthus nasutus. *Pharmacogn. Mag.* **2017**, *13*, 652–658. [CrossRef]
45. Noshad, M.; Behbahani, B.A.; Nikfarjam, Z.; Zargari, F. Antimicrobial activity between *Coriandrum sativum* seed and *Cuminum cyminum* essential oils against foodborne pathogens: A multi-ligand molecular docking simulation. *LWT* **2023**, *185*, 115217. [CrossRef]
46. Sumera; Anwer, F.; Waseem, M.; Fatima, A.; Malik, N.; Ali, A.; Zahid, S. Molecular Docking and Molecular Dynamics Studies Reveal Secretory Proteins as Novel Targets of Temozolomide in Glioblastoma Multiforme. *Molecules* **2022**, *27*, 7198. [CrossRef] [PubMed]
47. Shakibay Senobari, Z.; Masoumian Hosseini, M.; Teimouri, M.B.; Rezayan, A.H.; Samarghandian, S.; Hekmat, A. Chromone-embedded peptidomimetics and furopyrimidines as highly potent SARS-CoV-2 infection inhibitors: Docking and MD simulation study. *BMC Res. Notes* **2023**, *16*, 224. [CrossRef] [PubMed]
48. Baranauskaite, J.; Ockun, M.A.; Uner, B.; Tas, C.; Ivanauskas, L. Effect of the Amount of Polysorbate 80 and Oregano Essential Oil on the Emulsion Stability and Characterization Properties of Sodium Alginate Microcapsules. *Molecules* **2021**, *26*, 6304. [CrossRef]
49. García-Armenta, E.; Picos-Corrales, L.A.; Gutiérrez-López, G.F.; Gutiérrez-Dorado, R.; Perales-Sánchez, J.X.K.; García-Pinilla, S.; Reynoso-García, F.; Martínez-Audelo, J.M.; Armenta-Manjarrez, M.A. Preparation of surfactant-free emulsions using amaranth starch modified by reactive extrusion. *Colloids Surf. A Physicochem. Eng. Asp.* **2020**, *608*, 125550. [CrossRef]
50. Marín, I.; Sayas-Barberá, E.; Viuda-Martos, M.; Navarro, C.; Sendra, E. Chemical Composition, Antioxidant and Antimicrobial Activity of Essential Oils from Organic Fennel, Parsley, and Lavender from Spain. *Foods* **2016**, *5*, 18. [CrossRef]
51. Zhang, R.; Wang, X.W.; Liu, L.; Cao, Y.C.; Zhu, H. Dietary oregano essential oil improved the immune response, activity of digestive enzymes, and intestinal microbiota of the koi carp. *Cyprinus carpio*. *Aquaculture* **2020**, *518*, 734781. [CrossRef]
52. Shah, M.A.; Jakkawanpitak, C.; Sermwittayawong, D.; Panichayupakaranant, P. Rhinacanthins-rich Extract Enhances Glucose Uptake and Inhibits Adipogenesis in 3T3-L1 Adipocytes and L6 Myotubes. *Pharmacogn. Mag.* **2018**, *13*, S817–S821. [CrossRef]
53. Van, C.K.; Nguyen, P.T.N.; Nguyen, T.T.T.; Bach, L.G. Microencapsulation of Citrus latifolia peel essential oil by spray-drying using maltodextrin: Characterization, antimicrobial activities, and release profile. *LWT* **2024**, *197*, 115825. [CrossRef]
54. Yang, J.L.; Liu, D.X.; Jiang, H.; Pan, F.; Ho, C.S.; Ho, R.C. The Effects of High-fat-diet Combined with Chronic Unpredictable Mild Stress on Depression-like Behavior and Leptin/LepRb in Male Rats. *Sci. Rep.* **2016**, *6*, 35239. [CrossRef] [PubMed]
55. Parasuraman, R.; Jayamurali, D.; Manoharan, N.; Govindarajalu, S.N. Neuroprotective effect of bromelain on BDNF-TRKB signalling pathway in chronic unpredictable stress-induced depression model. *Beni-Suef Univ. J. Basic Appl. Sci.* **2024**, *13*, 21. [CrossRef]
56. Asadi, K.; Abbasi-Maleki, S.; Sadeghi Hashjin, G. Antidepressant-like effect of *Cuminum cyminum* essential oil on the forced swim and tail suspension tests in male mice. *J. Shahrekord Univ. Med. Sci.* **2020**, *22*, 167–172. [CrossRef]
57. Haque, M.; Ansari, H. Anti-Obesity Effect of Arq Zeera and Its Main Components Thymol and Cuminaldehyde in High Fat Diet Induced Obese Rats. *Drug Res.* **2018**, *68*, 637–647. [CrossRef] [PubMed]
58. Kang, N.H.; Mukherjee, S.; Min, T.; Kang, S.C.; Yun, J.W. Trans-Anethole Ameliorates Obesity via Induction of Browning in White Adipocytes and Activation of Brown Adipocytes. *Biochimie* **2018**, *151*, 1–13. [CrossRef]
59. Abbasi-Maleki, S.; Maleki, S.G. Antidepressant-like effects of *Foeniculum vulgare* essential oil and potential involvement of dopaminergic and serotonergic systems on mice in the forced swim test. *PharmaNutrition* **2021**, *15*, 100241. [CrossRef]
60. Hassanzadeh, S.A.; Abbasi-Maleki, S.; Mousavi, Z. Anti-depressive-like effect of monoterpene trans-anethole via monoaminergic pathways. *Saudi J. Biol. Sci.* **2022**, *29*, 3255–3261. [CrossRef]

61. Rostami-Faradonbeh, N.; Amini-Khoei, H.; Zarean, E.; Bijad, E.; Lorigooini, Z. Anethole as a promising antidepressant for maternal separation stress in mice by modulating oxidative stress and nitrite imbalance. *Sci. Rep.* **2024**, *14*, 7766. [CrossRef]
62. Azmi, N.H.; Ismail, N.; Imam, M.U.; Ooi, D.J.; Oslan, S.N.H. Modulation of High-Fat Diet-Induced Brain Oxidative Stress by Ferulate-Rich Germinated Brown Rice Ethyl Acetate Extract. *Molecules* **2022**, *27*, 4907. [CrossRef]
63. Felger, J.C.; Haroon, E.; Patel, T.A.; Goldsmith, D.R.; Wommack, E.C.; Woolwine, B.J.; Le, N.A.; Feinberg, R.; Tansey, M.G.; Miller, A.H. What Does Plasma CRP Tell Us about Peripheral and central Inflammation in Depression. *Mol. Psychiatry* **2020**, *25*, 1301–1311. [CrossRef] [PubMed]
64. Deng, H.; Tian, Z.; Zhou, H.; Zhang, Y.; Chen, X.; Cui, Y.; Aifeire, A.; Zhang, X.; Wei, Z.; Shen, P.; et al. Elucidating the effects of cumin (*Cuminum cyminum*) fruit and stem as feed additives on growth, antioxidant capacity, liver and intestinal health, and gut microbiome of Nile tilapia (*Oreochromis niloticus*). *Aquac. Rep.* **2023**, *31*, 101687. [CrossRef]
65. Li, X.H.; Liu, L.; Wu, W.Z. Trans-Anethole Alleviates DSS-Induced Ulcerative Colitis by Remodeling the Intestinal Flora to Regulate Immunity and Bile Acid Metabolism. *Mediat. Inflamm.* **2023**, *2023*, 4188510. [CrossRef]
66. de Morais, S.V.; Calado, G.P.; Carvalho, R.C.; Garcia, J.B.S.; de Queiroz, T.M.; Cantanhede Filho, A.J.; Lopes, A.J.O.; Cartágenes, M.d.S.d.S.; Domingues, G.R.d.S. Impact of Cuminaldehyde and Indomethacin Co-Administration on Inflammatory Responses in MIA-Induced Osteoarthritis in Rats. *Pharmaceuticals* **2024**, *17*, 630. [CrossRef]
67. Yu, C.; Wang, D.; Li, Q.; Tong, Y.; Yang, Z.; Wang, T. Trans-anethole ameliorates LPS-induced inflammation via suppression of TLR4/NF-κB pathway in IEC-6 cells. *Int. Immunopharmacol.* **2022**, *108*, 108872. [CrossRef]
68. Chen, Q.; Gan, Z.; Zhao, J.; Wang, Y.; Zhang, S.; Li, J.; Ni, Y. In vitro comparison of antioxidant capacity of cumin (*Cuminum cyminum* L.) oils and their main components. *LWT-Food Sci. Technol.* **2014**, *55*, 632–637. [CrossRef]
69. Mohamed, M.E.; Kandeel, M.; Abd El-Lateef, H.M.; El-Beltagi, H.S.; Younis, N.S. The Protective Effect of Anethole against Renal Ischemia/Reperfusion: The Role of the TLR2,4/MYD88/NFκB Pathway. *Antioxidants* **2022**, *11*, 535. [CrossRef]
70. Yin, H.; Zhang, Q.; Li, Y.; Ma, J. Prevalence and correlates of severe anxiety in patients with first hospitalization for major depressive disorder combined with dyslipidemia: A large sample cross-sectional study. *Front. Psychiatry* **2024**, *14*, 1289614. [CrossRef]
71. Wang, S.; Gao, X.; Li, P.; Liu, S.; Zeng, Y. Chronic unpredictable mild stress combined with a high-fat diets aggravates atherosclerosis in rats. *Lipids Health Dis.* **2014**, *13*, 77. [CrossRef]
72. Jia, Q.; Yang, H.; Zhuang, N.; Yin, X.; Zhu, Z.; Yuan, Y.; Yin, X.; Wang, Y.; Cheung, E.F.C.; Chan, R.C.K.; et al. The role of lipoprotein profile in depression and cognitive performance: A network analysis. *Sci. Rep.* **2020**, *10*, 20704. [CrossRef]
73. Han, A.L. Association between lipid ratio and depression: A cross-sectional study. *Sci. Rep.* **2022**, *12*, 6190. [CrossRef]
74. Lin, P.Y.; Chang, A.Y.; Lin, T.K. Simvastatin treatment exerts antidepressant-like effect in rats exposed to chronic mild stress. *Pharmacol. Biochem. Behav.* **2014**, *124*, 174–179. [CrossRef] [PubMed]
75. Samadi-Noshahr, Z.; Hadjzadeh, M.A.; Moradi-Marjaneh, R.; Khajavi-Rad, A. The hepatoprotective effects of fennel seeds extract and trans-Anethole in streptozotocin-induced liver injury in rats. *Food Sci. Nutr.* **2021**, *9*, 1121–1131. [CrossRef]

Disclaimer/Publisher's Note: The statements, opinions and data contained in all publications are solely those of the individual author(s) and contributor(s) and not of MDPI and/or the editor(s). MDPI and/or the editor(s) disclaim responsibility for any injury to people or property resulting from any ideas, methods, instructions or products referred to in the content.